APPENDIX B.

MODELING THE POTENTIAL EFFECTS OF CHANGED WATER AVAILABILITY, WATER TEMPERATURE, AND SEA LEVEL RISE ON PACIFIC SALMON CULTURE PROGRAMS AT MAKAH NATIONAL FISH HATCHERY

Kyle C. Hanson[1] and Douglas P. Peterson[2]

US Fish and Wildlife Service, Abernathy Fish Technology Center,

1440 Abernathy Creek Road, Longview, WA 98632

Original Draft: October 4, 2016

[1] Current address: Columbia River Fish and Wildlife Conservation Office, U.S. Fish and Wildlife Service, 1211 S.E. Cardinal Court, Suite 100, Vancouver, WA 98633. Email: Kyle_Hanson@fws.gov.

[2] Email: Doug Peterson@fws.gov

ABSTRACT

Future climate conditions may impede the ability of salmon hatcheries in the Pacific Northwest to operate under a 'business as usual' paradigm with current rearing schedules and fish production targets. Here, we evaluate the vulnerability of the current Chinook salmon (*Oncorhynchus tshawytscha*), coho salmon (*O. kisutch*), and steelhead (*O. mykiss*) programs at Makah National Fish Hatchery (NFH) to future climates expected by the 2040s under a suite of 10 global circulation models (GCM) forced by the 'middle-of-the-road' A1B greenhouse gas emissions scenario. We summarize projected environmental conditions in the Tsoo-Yess River basin in western Washington State and then use those data to implement a temperature-driven growth model for hatchery-reared salmon and steelhead that allowed us to evaluate temporal changes in mean fish size, water *flow index*, and fish *density index*. By the 2040s, the Tsoo-Yess River, the only water source for fish culture at Makah NFH, is expected to be warmer in all months, and fish in each program will experience mean monthly temperatures 1.0 – 2.4°C greater than the historical average. Our modeling projects that juvenile Chinook salmon reared at the facility will be 15-30% heavier and 5-9% longer in most months. Similarly, coho salmon are projected to be 30-42% heavier and 6-12% longer in most months, and steelhead are projected to be 30-40% heavier and 9-12% longer. By the 2040s, the Tsoo-Yess River is projected to experience higher average flows and more frequent large floods in winter, and lower average flows and more frequent droughts in summer.

With a 'business as usual' fish culture approach, warmer stream temperatures will result in larger fish in all months for all three programs at Makah NFH, but the overall effect of climate change on each program depends strongly on the life-history rearing schedule for each species. Impacts to the Chinook salmon program will likely be comparatively moderate because juvenile rearing at the hatchery occurs for only a few months, from late fall to early spring. In contrast, the two programs that include rearing of fish during the summer months – coho salmon and steelhead – will be increasingly challenged by the anticipated future conditions because the predicted future temperatures are expected to meet or exceed the physiological optima for each species. Coho salmon and steelhead already face significant problems with disease outbreaks during years with high temperatures and/or lower water availability. The environmental conditions that have led to previous outbreaks of disease are expected to be more frequent and severe by the 2040s, and the period of high susceptibility to disease is predicted to expand so that it covers nearly half the year (June-October). Increases in flow and density index values are projected to approach or exceed existing fish-health guideline during summer months, further indicative of future conditions (e.g., crowding, reduced water quality) that would promote an outbreak of disease in a hatchery setting. The existing water re-use strategy, whereby hatchery effluent is recirculated through a bypass channel, was not explicitly accounted for in our models (we had to assume a high-quality water source), so we may have underestimated the *effective* flow index values during summer months for raceways supplied with recirculated water.

Mitigation of anticipated climate effects on salmon culture – especially for effects of increased stream temperatures – is theoretically possible at Makah NFH but may require multiple, concurrent strategies (e.g., chilling water and reduced food rations) that would require cost-benefit analyses to determine feasibility. Reducing rearing densities may reduce crowding, but this would not alleviate prevailing environmental constraints (temperature, water availability) that are anticipated to become more severe by the 2040s. The existing water-recirculation strategy warrants evaluation given the potential for reduced water quality and recent disease outbreaks at the hatchery, although climate change may impose additional limitations on the efficacy of this latter approach.

INTRODUCTION

Pacific salmon (*Oncorhynchus* spp.) have a complicated life cycle and may be sensitive to effects of climate change through a number of pathways. Changes in air temperature and precipitation patterns may cause freshwater rearing habitat to become unsuitable because of altered thermal and hydrologic regimes (Mantua et al. 2010). Increased fire frequency and duration in the western U.S. (e.g., Westerling et al. 2006) may alter disturbance regimes and influence the structure and function of some aquatic systems (e.g., Bisson et al. 2003; Isaak et al. 2010). Temperature increases in mainstem rivers can create seasonal thermal migration barriers that block adults from reaching spawning habitats (Mantua et al 2010). The establishment of new invasive species, spread of existing ones that compete with Pacific salmon, and their impacts will depend, to some extent, on how freshwater habitats are affected by climate change (Petersen and Kitchell 2001; Rahel and Olden 2008; Carey et al. 2011). Changes in ocean temperature, upwelling (e.g., Scheuerell and Williams 2005), and acidification (e.g., Fabry et al. 2008) could dramatically alter the food webs in the marine ecosystems on which salmon depend during the ocean phases of their life cycle.

The viability of wild (naturally spawning) and propagated (hatchery-reared) populations of Pacific salmon could be affected by some or all of the aforementioned factors, but a comprehensive analysis of all those factors and effects is beyond the scope of the effort described here. Rather, our intent is to focus in significant detail on one portion of the life cycle of hatchery-propagated salmon – that portion which takes place in the hatchery – and understand specifically how growth rates, mean size, and total biomass during that freshwater phase are affected by changes in water availability and temperature anticipated under climate change. This emphasis is based on two premises. First, the freshwater rearing phase of the salmon's life cycle could represent a population bottleneck if climatic changes result in conditions that meet or

exceed a species' physiological tolerances. This premise should be valid whether the rearing phase occurs in a hatchery or in a natural setting. Second, hatchery managers have some ability to influence rearing conditions within the hatchery. The hatchery represents an environment, albeit artificial, over which the USFWS has scope to directly design and implement climate mitigation and adaptation strategies.

Given these premises, our overall objective is to understand whether hatchery programs can operate in a 'business as usual' paradigm following existing rearing schedules and production targets under future climatic conditions, focusing specifically on changes in water temperature and water availability at the hatchery. Specific objectives are to: (a) determine if future environmental conditions are likely to altogether preclude propagation of certain species, (b) identify the magnitude and timing of sub-lethal effects that may affect freshwater growth and survival of each species, including the incidence of disease; and (c) suggest general mitigation strategies given the sensitivities detected in (a) and (b). To do this, we collated – from the scientific literature – physiological tolerance data for Pacific salmon species of interest, adapted a temperature-driven growth model to predict fish growth, and developed a modeling framework using flow index and density index parameters (Piper et al. 1982; Wedemeyer 2001) which integrate the effects of changing water temperature and availability within the Makah NFH. We briefly summarize the important hydrologic changes anticipated for the Tsoo-Yess River basin upstream from the hatchery. We then use empirical data on recent fish-rearing conditions at the hatchery to predict the future growth and total mean weights (biomass) of each of three species (Chinook salmon, coho salmon, and steelhead) currently propagated at Makah NFH by (a) implementing the growth model and then (b) modeling flow and density indices based on in-

hatchery environmental conditions predicted for the 2040s under one greenhouse gas scenario (A1B) and incremental changes in water temperature and availability.

METHODS

Salmon thermal tolerances

In August 2011, a review of the peer reviewed literature of thermal tolerances of five focal species of Pacific salmon and trout (Chinook, coho, chum, and sockeye salmon, and steelhead) reared at National Fish Hatcheries (NFH's) in the Pacific Northwest was performed to determine the thermal tolerances for multiple life-history stages. This information was acquired though two general approaches. First, to identify relevant primary literature, ISI's Web of Science (1985-present) was searched for variations on the following key terms: *thermal tolerance*, *critical thermal maximum* (CTM), *incipient lethal temperature* (ILT), *temperature maximum* (TL), and *ultimate lethal incipient temperature* (UILT). Second, bibliographies from several reviews of thermal tolerance in fishes (Beitinger et al. 2000; Becker and Genoway 1979; Paladino et al. 1980; Beitinger and McCauley 1990; Lutterschmidt and Hutchinson 1997) were surveyed to locate additional information on each focal species. Results were then screened for relevance before inclusion in the literature review, and studies that did not specifically contain information on the thermal tolerance of the focal species were excluded from further synthesis. We attempted to extract the following thermal tolerance data (Elliott 1981) from results, tables and figures:

1. *Optimal temperatures*: the temperature range that allows for normal physiological response and behavior without thermal stress symptoms;
2. *Optimal growth temperatures*: the temperature range that provides the highest growth rates given a full food ration;

3. *Optimal spawning temperatures*: the temperature range that results in lowest pre-spawn mortality and the highest fertilization rates and egg survival;
4. *Upper smoltification temperature limit*: the minimum, upper temperature at which the smoltification process is inhibited;
5. *CTM, ILT, or UILT*: the maximum temperature that induces 50% mortality in the fish previously acclimated to a given constant temperature.

Meta-data available varied among publications, but to the extent possible, the following variables were recorded for each datum: species, life-history stage, fish length (mean ± SD or range in mm), fish weight (mean ± SD or range in g). The following supplemental meta-data from published values of CTM or ILT tests was also recorded, when provided, to facilitate proper interpretation of results: acclimation temperature (°C), maximum temperature from CTM or ILT tests (°C), and test endpoint criterion. Thermal tolerance data were categorized by the following three life-history stages: egg/fry, juvenile, and adult broodstock.[3] Data were averaged for each of the three life-history stages to determine representative thermal tolerances for each species at each life-history stage (Table B1).

Disease thermal tolerances

In August, 2011, we reviewed the peer reviewed scientific literature on thermal tolerances of common pathogens that infect salmon at aquaculture facilities in the Pacific Northwest to determine the range of temperatures at which each species of pathogen is known to cause disease in salmon. The literature review followed the same protocols as described above, but with the common names or Latin binomial names of pathogens added to the following search

[3] These three life-history stages are the principle ones addressed by salmon hatcheries in the Pacific Northwest. Egg/fry include fertilized eggs, sac fry, and fish less than 70 mm total length. Juvenile fish are sexually immature fish in large rearing containers (e.g., raceways) prior to release. Adult broodstock are sexually mature fish that have returned to the facility during the spawning migration.

terms: *thermal tolerance*, *outbreak temperature*, and *transmission temperature*. Results were then screened for relevance before inclusion in the literature review, and studies that did not specifically contain information on the thermal tolerance of the focal species were excluded from further synthesis. A total of four citations provided detailed information on the following two variables (Table B2):

1. *Disease outbreak temperatures*: The pathogen-specific temperature range at which disease and mortality are most likely in Pacific salmon and steelhead; and
2. *Minimum disease temperatures*: The lowest temperature (or range) at which the pathogen-specific disease occurs in Pacific salmon and steelhead.

Fish rearing conditions at Makah NFH: water temperatures

We were not able to obtain a long-term dataset of water temperatures at Makah NFH, either for the hatchery or for the Tsoo-Yess River. The Tsoo-Yess River has a USGS streamflow gage downstream from the confluence with Miller Creek, but this particular station[4] does not record stream temperature. We tried to obtain historical stream temperatures by conducting data calls with staff from Makah NFH, the USFWS Western Washington Fish and Wildlife Conservation Office in Lacey, WA (that works closely with Makah NFH), and biologists with the Makah Tribe. Apparently, few long-term temperature records exist, or if they do exist, their whereabouts are unknown.

Despite the apparent absence of long-term temperature records at Makah NFH, we were able to obtain two summarized datasets. (1) Dataset 1 consisted of the average daily water temperature for each day of the year (e.g., January 1, January 2, …, December 31, excluding February 29) averaged over eight consecutive years, 1982-1989, to yield 365 temperature data

[4] (http://waterdata.usgs.gov/nwis/uv?site_no=12043163)

points for that time period. Those average daily temperatures (1982-1989) ranged from 39ºF (December 27) to 66ºF (August 8). (2) Dataset 2 consisted of the average daily water temperatures recorded with digital thermistors (HOBO loggers) at raceways in Makah NFH each day during the six year period, 2010-2015, to yield approximately 2,200 temperature data points for that time period. We then calculated average temperatures for each month for each of those two datasets and time periods. Based on those calculations, average water temperatures in1982-1989 were slightly warmer in the spring and summer than during 2010-2015, which translated to a 0.5ºC difference in mean annual water temperature (Figure B1, panel A). This latter difference should be interpreted cautiously because the methods for collecting the data in Dataset 1 are unknown. In addition, the underlying data in each dataset were pooled and averaged within months and across years differently. Overall, the temperature values in the two datasets were quite similar, and we ultimately used Dataset 1 (the 1982-1989 data) as the baseline thermal-rearing conditions for fish reared in Makah NFH because this latter approach facilitated the modeling of future temperatures (see below).

Projected thermal conditions at Makah NFH during the 2040s

To estimate future surface water temperatures in the Tsoo-Yess River near Makah NFH, we established a regression relationship between recent air and water temperature using the method of Mohseni et al (1989). We then used air temperatures predicted for the 2040s under the A1b greenhouse gas emissions scenario (IPCC 2007) to generate water temperature predictions for the 2040s based on the aforementioned regression model. The non-linear regression model of Mohseni et al. (1998) uses the equation,

$$T_{sw} = \mu + \frac{\alpha + \mu}{1 + e^{\gamma(\beta - T_{air})}}$$

where T_{sw} = surface water temperature, μ = estimated minimum stream temperature, α = estimated maximum stream temperature, γ = a measure of the steepest slope of the function, β = the air temperature at the inflection point of the function, and T_{air} = measured air temperature. We followed the approach of Mantua et al. (2010) to establish a site-specific relationship between weekly air and water temperatures. Mean weekly air temperature for the Tsoo-Yess River watershed (upstream from Makah NFH) was estimated from modeled historical data[5] as the area-weighted average of mean daily temperatures overlap between 1/16-degree grid cells and the watershed boundary delineated using a Geographic Information System (GIS). These weighted, weekly air temperatures were then fitted to mean weekly water temperatures from the 1982-1989 time period. The modeled historical air temperature data covers a time period 1915-2006, but we did not use this entire time period to fit the regression model. For consistency with the available water temperature data, we extracted the air temperature data for 1982-1989, and then calculated daily and weekly averages over that entire time period. We then used those data to fit the model estimated by the Nash-Sutcliffe coefficient (NSC) (Nash and Sutcliffe 1970), assuming a stationary relationship between weekly average air and surface water temperatures. We fit the model with the non-linear regression package 'nls' in R version 3.2.3 (R Core Team 2015). The regression model for Tsoo-Yess River temperatures provided an excellent fit with a Nash-Sutcliffe efficiency coefficient (NSC) of 0.966 which yielded the following parameterized equation:

$$T_{sw} = 3.21 + \frac{24.61 + 3.21}{1 + e^{0.23(12.56 - T_{air})}}$$

[5] Flux files from: http://warm.atmos.washington.edu/2860 .

Surface water temperature (T_{SW}) predictions for the 2040s were generated by applying the statistically downscaled air temperature predictions from an ensemble of 10 general circulation models (GCM's) – ccsm3, cgcm3.1_t47, cnrm_cm3, echam5, echo_g, hadcm, hadgem1, ipsl_cm4, miroc_3.2, and pcm1 – forced by the A1B emissions scenario (IPCC 2007; Hamlet et al. 2010a,b). The A1B scenario is often referred to as "middle-of-the-road" in terms of greenhouse gas emissions levels and projected atmospheric warming, and has been utilized as a reference in many studies (e.g., Mantua et al. 2010; Wenger et al. 2011*).* The A1B scenario also assumes that some global efforts are undertaken in the 21st Century to reduce the rate of increase in greenhouse gas emissions compared to the 1980 - 1999 baseline established in the 4th IPCC Assessment Report (IPCC 2007).[6]

The modeled 2040s A1B water temperatures were used to simulate the monthly thermal conditions experienced by fish reared in Makah NFH. The historical and future modeled temperatures exhibited unexpected fluctuations in the January-March time period, rather than steady warming (Figure B1, panel B); this was apparently an artefact of the underlying climate flux files for that specific geographic location. Consequently, predicted water temperature

[6] The A1B scenario and other global model outputs of the 4th IPCC (IPCC 2007) have recently been supplanted by a new set of scenarios and modeled outputs from the 5th IPCC (IPCC 2014). The A1B is referred to as a SRES scenario described in the Intergovernmental Panel on Climate Change (IPCC) Special Report on Emissions Scenarios (IPCC 2000). A1B is one of a family of scenarios used in fourth global climate assessment (AR4) that describe greenhouse gas emissions under alternative developmental pathways assuming different future expectations for demographic, economic, and technological outcomes with no additional climate policies (IPCC 2007). The most recent IPCC global climate assessment (AR5) uses a different methodology to describe global climate forcing, called Representative Concentration Pathways or RCPs (IPCC 2014). The RCPs represent trajectories for greenhouse gas emissions and other atmospheric elements that affect the radiative forcing of the earth's climate through time and assume possible mitigation actions (van Vuuren et al. 2011). The AR5 assessment uses four representative RCPs: RCP2.6, RCP4.5, RCP6, and RCP8.5 in rank order of their radiative forcing and emission levels (van Vuuren et al. 2011; IPCC 2014). The SRES A1B scenario falls roughly between the RCP6 and RCP8.5 (though closer to RCP6) in terms of CO_2 concentration, radiative forcing, and expected increases in mean global temperatures (van Vuuren and Carter 2014). We acknowledge the updated and improved assessments of AR5 (IPCC 2014) but have relied here on the outputs of the A1B scenario of AR4 (IPCC 2007) for our vulnerability assessment of Makah NFH to maintain quantitative consistency with our previous and other ongoing vulnerability assessments of NFHs in the Pacific Northwest.

values for the 2040s were calculated by incrementing the selected empirical historical values (Figure B1, panel A, dotted line) with the difference between the modeled historical and future values (Figure B1, panel B). Those water temperature predictions were then used in subsequent modeling (e.g., fish growth model) and presented in Figure B2 and Table B3.

Growth model simulation

We used the fish growth model of Iwama and Tautz (1981) to estimate how the growth of hatchery-reared Chinook salmon, coho salmon, and steelhead might change in response to future climates. This model has been widely applied to evaluate growth of captive salmonids (Dumas et al. 2007; Good et al. 2009; Jobling 2010), and we used it here to estimate mean fish size at age (month of year) as a function of water temperature assuming unlimited food ration. We solved the equation to estimate mean fish weight at time-step i (W_i) as:

$$W_i = \left[W_0^b + \left(\frac{T_i}{10^3} \right) \bullet d_i \right]^{\frac{1}{b}}$$

where W_0, is initial weight (g), and T_i and d_i are the average temperature and number of days in time-step "i". Iwama and Tautz (1981) analyzed growth data for three species of salmonid fishes and proposed $b = 0.33$ as a reasonable approximation that balanced model accuracy and simplicity; consequently, we applied that exponent in our analyses.

To estimate mean fish length (L_i) by time-step, we rearranged an equation for Fulton-type fish condition factor (Anderson and Gutreuter 1983) to solve for fish fork length (L_i in mm) as:

$$L_i = \left(\frac{W_i}{K / 10^5} \right)^{1/3}$$

where *K* is the condition factor which was held constant at K = 1.0 to represent fish in a healthy condition.

We applied the growth model to estimate monthly fish sizes of Chinook salmon, coho salmon, and steelhead after transfer (aka "ponding") to outside raceways. The initial weight at ponding was the input for the first month in the growth simulation, and subsequent months were initialized using the predicted final weight of the fish from the preceding month. The growth model was implemented with hatchery thermal environments consistent with (a) recent historical conditions and (b) those projected for the 2040s. We then compared cumulative differences in mean size of the fish for each species between those two thermal regimes.

Projected water availability and sea level rise at Makah NFH during the 2040s

To generate estimates for water availability at Makah NFH under the A1B emissions scenario, we used simulated streamflow data from the variable infiltration capacity (VIC) hydrologic model (Liang et al. 1994) forced by output from the same 10 GCM ensemble used to derive water temperatures (e.g., Mantua et al. 2010). Streamflow data were summarized as mean monthly surface water discharge in the Tsoo-Yess River routed to the location of Makah NFH (A. Hamlet, Climate Impacts Group, University of Washington, unpublished data). We assumed that the water available to the hatchery from all sources would change in direct proportion to the change in mean monthly flow estimated by the VIC model for the 2040s. The projected flow of water into the hatchery during the 2040s was estimated by multiplying (a) the modeled change in mean monthly flow, estimated as the ratio of VIC modeled historical and 2040s flows, by (b) the average monthly water used during the time periods 2010-2014 for Chinook salmon, 2010-2013 for coho salmon, and 2011-2014 for steelhead. For example, if the coho salmon program used 15 cfs on average during a hypothetical month, and the hydrologic model predicted that the mean

monthly discharge would decline by 40% in the 2040s, then the estimated water available for rearing coho salmon in that month would be 9 cfs (15 cfs × 0.60). Additionally, we assumed the hatchery cannot utilize additional water (above the mean historical use) in months where an increase in mean flow was projected.

The impact of sea level rise (SLR) was not explicitly modeled for this report because detailed projections for the geographic area adjacent to Makah NFH are not currently available. However, the rate of SLR has been estimated for other locations nearby (e.g., Neah Bay and Puget Sound). Models for Western Washington (e.g., Mote et al. 2008; Huppert et al. 2009) have utilized estimates of future, *relative* SLR for the years 2050 and 2100 under multiple global climate models (see Mote et al. 2008 for details). These estimates included integrating three modeled levels of future global SLR (very low [16 cm], medium [34 cm], and very high [128 cm] by 2100) driven by (a) eustatic SLR caused by expanding volume of the ocean due to warming, (b) melting glaciers, sea ice and polar ice caps (including Greenland), (c) local rates of vertical land movement along the coastline of Washington State due to plate tectonics and geologic subsidence, and (d) seasonal wind-driven increases in sea level (Snover et al. 2007; Mote et al. 2008; Huppert et al. 2009). Rates of local SLR in Washington and Oregon (NRC 2012) are similar to those projected by Mote et al. (2008), indicating that the downscaled SLR estimates for Neah Bay in 2050 would provide the best surrogate estimate for SLR at the mouth of the Tsoo-Yess River and Makah NFH.

Flow index and density index: critical fish culture parameters

Hatcheries typically operate to achieve a production target (mean weight and total number of fish at release) while remaining below flow and density index values established as fish health guidelines based on empirical observations of fish disease, mortality, and poor growth

when fish are overcrowded. These indices essentially function as general rules of thumb based on oxygen saturation for different water temperatures and elevation (e.g., Piper et al. 1982), and they act as surrogates for carrying capacity within the facility. Conceptually, these indices are the total fish biomass divided by the product of the mean fish length and (a) water use (flow index) or (b) rearing capacity (density index):

$$FI_i = \frac{N_i \bullet W_i}{L_i \bullet GPM_i}$$

and

$$DI_i = \frac{N_i \bullet W_i}{L_i \bullet C_i}$$

where FI_i and DI_i are flow and density indices, respectively, N_i is the total number of fish (abundance), W_i is mean fish weight (lb.), L_i is mean fish length (in), GPM_i is water use rate by the hatchery (gallons per min), and C_i is the rearing capacity (ft^3) at monthly time-step i. In this formulation, mean fish length (L_i) and weight (W_i) are forced by water temperature (T_i), which thus links temperature (and climate) changes to variation in FI_i and DI_i. Flow index also changes in response to water availability (GPM_i). Rearing capacity (C_i) does not necessarily change in response to climate, but operationally, it could be adjusted by managers (e.g., build more raceways) to compensate for the effect of increased fish growth on DI_i.

Integrating the effect of water temperature and water availability on hatchery operations

We utilized flow and density indices to integrate the effect of changing water temperatures, water availability, and rearing capacity[7] using two approaches to represent variation in climate

[7] In general, hatchery rearing capacities were used as surrogates for biological carrying capacity under historical and future conditions.

and rearing conditions. First, we used both recent historical conditions and climate model output for the 2040s to drive the salmon growth model and to simulate flow and density indices for each species in each monthly time-step after initial ponding. This produced two monthly values for each index at each time-step (modeled historical and modeled future values). The modeled historical and empirical FI_i and DI_i values recorded in the hatchery could differ because of real-time changes implemented by hatchery managers, such as reducing feed rations or increasing hatchery water use in response to environmental conditions. We could not explicitly represent these factors in the analyses, so we adjusted the future simulated values based on the ratio between the empirical and modeled historical values (rFI_i and rDI_i) as:

$$rFI_i = \frac{FI_i \ mean\ empirical\ historical}{FI_i \ modeled\ historical}$$

$$rDI_i = \frac{DI_i \ mean\ empirical\ historical}{DI_i \ modeled\ historical}$$

Thus, the future bias-corrected index values were:

$$FI_i \ future\ corrected = rFI_i \bullet FI_i \ modeled\ future$$

$$DI_i \ future\ corrected = rDI_i \bullet DI_i \ modeled\ future$$

A complete description of the model formulation and underlying equations are presented in Hanson and Peterson (2014).[8]

[8] Note: $rDI_i = rFI_i$ (= r_i) at each time step because (a) the value of N_iW_i/L_i is the same for calculating DI_i and FI_i at each time step for each case (i.e., N_iW_i/L_i differs between modeled historical and empirical cases but not between DI_i and FI_i for each case), and (b) the values for GPM_i and C_i, respectively, at each time step were the same in both cases (i.e., the modeled historical case used the same values of GPM_i and C_i, respectively, as those measured empirically).

Second, we conducted a sensitivity analysis to examine how the flow and density indices changed based on incremental changes in temperature and water availability. For the flow index, we plotted monthly index values based on combinations of water temperature (100 increments covering historical mean temperature ± 4ºC) and water use (50 increments ranging from 40% to 150% of historical mean water utilization in cfs) to generate a monthly response surface of 5,000 points. We did the same for the density index but used incremental changes in capacity (50 increments ranging from 50% to 200% the historical mean). The generating equations for the sensitivity analyses are those for FI_i and DI_i presented above, with the appropriate substitutions for temperature and fish size.

RESULTS

Projected future climate at Makah NFH under the A1B emissions scenario

Under the A1B emissions scenario, the Tsoo-Yess River basin is projected to experience warmer air and stream temperatures, lower base flows in summer, higher flows in winter, and more extreme winter floods by the 2040s (Tables B3-B5; Figures B1-B8). Mean air temperature over the entire watershed is expected to increase in every month (mean = 1.7ºC, SD = 0.38ºC) with the largest absolute increases projected for July-September (range 2.2-2.4ºC; Table B4). Total annual precipitation is projected to be within 5% of the historical baseline (historical: 243 mm vs. 2040s: 256 mm) but to exhibit more pronounced seasonal differences with slightly less precipitation in summer and early fall (May-September) and slightly more in other months (Table B4). The Tsoo-Yess River has a rain-driven hydrology, and the modeling did not indicate substantial changes in the overall snow water equivalent (Table B4). There was an indication of reduced future snowpack in January, but the historical estimate is already quite small (Table B4). Based on the VIC modeling, mean annual flows projected for the Tsoo-Yess River in the 2040s

(mean 485 cfs, range 424-535 for 10 GCMs) will be slightly greater than the modeled historical values (454 cfs, Table B5; see also Figures B3-B4). The magnitude of seasonal flows, in contrast, is projected to be different in the future, with greater uncertainty about the increase in winter flows. Mean flows by the 2040s were projected to increase by an average of 7.2% (ensemble range 5.7% to 23.8%) in the late fall and winter (October-March) and decrease by an average of 19.1% (ensemble range -6.0% to -34.6%) in summer (June-September) (Figures B3 and B8). The shape of the hydrographs are generally similar for both historical and 2040s time periods (Figure B3), but in the future, the timing of the center in flow mass is earlier in the year (Figure B5), perhaps because of the projected increase in flows during winter months when flows are greatest. The severity of summer droughts may also increase (Figure B6). Large increases in the magnitude of large (100-year) winter floods are also predicted (Figure B7).

Water temperature in the 2040's, based upon the A1B scenario and statistical downscaling of GCMs, are expected to increase in the Tsoo-Yess River (Table B3; Figures B1, panel B and Figure B2). In all months, modeling predicts that Tsoo-Yess River surface water temperatures will increase from 1.0°C (January) to 2.4°C (July, August, and September) compared to the historical averages for the 1982-1989 period. The most significant changes in surface water temperatures are predicted to occur in July (+2.4°C), August (+2.4°C), and September (+2.4°C). Given the predicted alterations to surface water temperatures at Makah NFH, the water temperatures across the fish production cycle will change.

SLR across a range of scenarios through the 2040s will have limited or no impact on operations at Makah NFH, based on the predictions of Huppert et al. (2009). For the 'very low' global SLR estimate, the NW Olympic Peninsula experiences negative (-) 12 cm of vertical SLR relative to geologic uplift (Huppert et al. 2009). For the 'medium' global SLR estimate, the NW

Olympic Peninsula experiences 0 cm of relative, vertical SLR (Huppert et al. 2009). Only under the 'very high' global SLR scenario would this area experience positive SLR (35 cm) through the 2040s (Huppert et al. 2009). In general, SLR along the western Washington coast is mitigated by vertical land uplift that is driven by the Juan de Fuca oceanic plate subducting under the North American continental plate (Mote et al. 2008). While seawater inundation of the local area around Makah NFH may not be likely by 2050, flooding during storm events, seawater intrusion into freshwater aquifers, altered conditions in the nearshore environment, and modification of the freshwater lens from the Tsoo-Yess River may all occur as a result of local SLR (Huppert et al. 2009).

Chinook salmon program

Adult Chinook salmon returning to Makah NFH are typically captured between September and November and are maintained in holding ponds supplied with Tsoo-Yess River water until they are spawned. By the 2040s, water temperatures between September and November are predicted to increase by 1.3°C to 2.4°C with a predicted high, mean-monthly water temperature at the hatchery of 17.6°C during the broodstock holding period (Table B6; Figure B9). In September, the historical temperatures meet or exceed the optimal spawning temperatures for Chinook salmon (9.0 – 12.3°C) based on literature values (Table B1); hence, the projected increase in water temperatures by the 2040s increases the likelihood that adult Chinook salmon will experience physiological stress during holding and spawning in both September and October, especially for fish captured earlier during that time period.

Juvenile Chinook salmon reared in Makah NFH will be exposed to warmer rearing conditions by the 2040s, with increases in water temperature ranging between 1.0°C and 2.0°C projected across the rearing period (Table B6, Figure B10). The largest monthly increases in

temperature are predicted to occur during initial rearing in October (+2.0°C) as well as at the end of the rearing period in May (+1.9°C) (Table B6, Figure B10). By the 2040s, water temperatures are predicted to approach the physiological threshold for optimal temperature for incubation of eggs and hatched fry during October at Makah NFH (Table B1 and Figure B10). At the time of release the following June, the predicted future water temperature within the facility (17.7°C; see Figure B2) exceeds the upper limit for proper smoltification (14.0°C; Table B1). Water temperatures during several months are predicted also to increase into the range of temperatures where disease outbreaks are likely for common salmon pathogens (Table B2). Of particular concern is the observation that juvenile Chinook salmon reared at Makah NFH have been affected historically by pathogen outbreaks at the end of the rearing cycle in May. With water temperatures in May predicted to increase by 1.9 – 2.0°C in the 2040s, such outbreaks may become more prevalent.

While the predicted future (2040s) temperatures at Makah NFH may not consistently exceed physiological tolerances of Chinook salmon, warmer water temperatures will most likely result in increased growth of juvenile Chinook salmon (Table B7, Figure B11). The largest increases in mean fish weight and length are predicted to occur in May (warmest month) when mean fish weight is predicted to increase by 29.3%, and mean fish length is predicted to increase to 8.9% (Table B7, Figure B11). Due to the warmer thermal environment during the entire rearing period, Chinook salmon smolts from the Makah NFH are predicted – under current culture protocols - to be 29.3% heavier and 8.9% longer at release compared to historical sizes.

The model-based climate scenarios suggest Makah NFH will experience small-to-modest increases in flow index values for juvenile Chinook salmon during January-April (Table B8, Figure B12a) but large increase in May when the adjusted flow index value is projected to

approach the upper guideline value of 1.0 under current culture protocols (Figure B12a). Increased flow index values are primarily driven here by increased water temperatures and concomitant faster fish growth; water availability is projected to decline only slightly beginning in May. Density index values for Chinook salmon at Makah NFH are also expected to increase (Table B8, Figure B12b), with the predicted adjusted value for May exceeding the 0.2 guideline value.

Coho salmon program

Adult coho salmon returning to Makah NFH are typically captured between September and November and maintained in holding ponds supplied with Tsoo-Yess River until they are spawned. By the 2040s, water temperatures between September and November are predicted to increase by 1.3°C to 2.4°C with a high, mean monthly water temperature at the hatchery of 17.6°C during the broodstock holding period (Table B9; Figure B13). In September and October, water temperatures by the 2040s are predicted to exceed the optimal spawning temperatures for coho salmon (5.7 – 11.7°C) based on literature values (Table B1). As a result, adult coho salmon will likely experience physiological stress during holding and spawning by the 2040s.

Juvenile coho salmon reared in Makah NFH will be exposed to warmer rearing conditions by the 2040s, with increases in water temperature ranging between 1.0°C and 2.4°C projected across the rearing periods (Table B9, Figure B14). Increases of more than 2.0°C are projected for June (+2.0°C), July (+2.4°C), August (+2.4°C), September (+2.4°C), and October (+2.0°C) of the first rearing year (Table B9, Figure B14). By the 2040s, water temperatures at Makah NFH from June until September are predicted to exceed the optimal, physiological temperatures for juvenile coho salmon (Table B1 and Figure B14). At the time of release in

April, the predicted future water temperature at the hatchery (11.4°C) does not exceed the upper limit for proper smoltification (14.3°C; Table B1). Water temperatures exceeding 17°C, well within the temperature range when disease outbreaks are likely for several pathogens (Table B2), are predicted to occur during four months of the juvenile rearing stage (Figure B14). Additionally, warmer temperatures in July and August in the 2040s will likely increase disease and mortality risks in those months (Table B2). In the 2000's, coho juveniles were often affected by outbreaks of furunculosis when water temperatures at the facility increased above ~15°C, a period that generally lasted from June to early September. With the predicted increases in water temperatures in the 2040s, the temporal window for these outbreaks could expand to cover May and all of September.

In addition to exceeding physiological tolerances of coho salmon in some months, the predicted future (2040s) temperatures would also increase the growth of juvenile coho salmon under current culture protocols (Table B10, Figure B15). Increases in mean fish weight and length are predicted to occur in all months, with mean fish weight predicted to increase by up to 40.9%, and mean fish length predicted to increase up to 12.0% (Table B10, Figure B15). Due to the warmer thermal environment during the entire rearing period, coho salmon smolts from Makah NFH are predicted to be 40.9% heavier and 12.0% longer, on average, at release compared to historical sizes.

The model-based climate scenarios suggest that juvenile coho salmon at Makah NFH may experience moderate-to-large increases in flow index values through their rearing cycle (Table B11, Figure B16a). The largest increases were predicted for (a) August-September and (b) during the last three months of the rearing cycle when adjusted flow index values are expected to approach or exceed the upper guideline value of 1.0. Density index values are

predicted to increase in most months (Table B11, Figure B16b) and are expected to exceed the upper guideline value of 0.2 in four months: once in the late summer (September) and for three consecutive months at the end of the rearing cycle (February-April).

Steelhead program

Adult steelhead returning to Makah NFH are typically captured between November and January and maintained in holding ponds supplied with Tsoo-Yess River water until they are spawned. By the 2040s, water temperatures during this holding period are predicted to increase by 1.0°C to 1.27°C with a predicted high, mean monthly water temperature at the hatchery of 9.3°C during the broodstock holding period (Table B12; Figure B17). Those projected increases in temperatures by the 2040s are not expected to exceed the optimal spawning temperatures for steelhead (6.4 – 15.3°C) based on literature values (Table B1). As a result, adult steelhead will most likely not experience increased physiological stress during the adult holding period compared to historic conditions.

Juvenile steelhead reared in Makah NFH will be exposed to warmer rearing conditions by the 2040s, with projected increases in water temperature ranging between 1.0°C and 2.4°C (Table B12, Figure B18). Increases of more than 2.0°C are projected for June (+2.0°C), July (+2.4°C), August (+2.4°C), September (+2.4°C), and October (+2.0°C) of the first rearing year (Table B12, Figure B18). By the 2040s, water temperatures at Makah NFH are predicted to exceed the upper physiological threshold for optimal temperature for juvenile steelhead from June until September (Table B1 and Figure B18). During this time period, juvenile steelhead are predicted to be exposed to water temperatures exceeding 19°C in July (19.6°C) and August (20.5°C) (Table B1 and Figure B18). At the time of release in April, the future water

temperature at the hatchery (11.4°C) is predicted to remain below the upper limit for proper smoltification of steelhead (12.6°C; Table B1). Water temperatures exceeding 17°C, well within the temperature range when disease outbreaks are likely for several pathogens (Table B2), are predicted to occur during four months of the juvenile rearing period (Figure B18). Additionally, warmer temperatures in July and August in the 2040s will likely increase disease and mortality risks in these months (Table B2). During the 2000's, juvenile steelhead were often afflicted with outbreaks of *Ichthyophthirius* (Ich) when water temperatures at the facility were greater than ~13°C, a period that generally lasted from June to September. With the predicted increases in water temperatures in the 2040s, the temporal window for disease outbreaks could expand to cover May to October.

In addition to exceeding physiological tolerances of steelhead in some months, the predicted future (2040s) temperatures would also increase the growth of juvenile steelhead under current culture protocols (Table B13, Figure B19). Increases in mean fish weight and length are predicted to occur in all months, with mean fish weight predicted to increase by up to 42.4%, and mean fish length predicted to increase up to 12.4% (Table B13, Figure B19). Due to the warmer thermal environment during the entire rearing period, steelhead smolts from the Makah NFH are predicted to be 42.3% heavier and 12.3% longer, on average, at release compared to historical sizes.

The model-based climate scenarios suggest that juvenile steelhead at Makah NFH may experience moderate-to-large increases in flow index values through their rearing cycle (Table B14, Figure B20a). The largest increases were predicted in late summer – driven by increases in fish size and reduced water availability – with predicted values exceeding the upper guideline value of 1.0 during August and September (Figure B20a). Adjusted density index values were

predicted to increase throughout the rearing cycle (Table B14, Figure B20b), and exceed the upper guideline value of 0.2 in six of 14 months. The months of greatest risk are August and September and during the last four months of the rearing cycle (February-May). The high densities in August and September occur before steelhead are tagged (coded wire tags) and redistributed to twice the number of raceways that they were held prior to tagging, thereby lowering density indexes substantially.

DISCUSSION

Warmer water and lower summer water availability at Makah NFH

Climate warming and hydrologic changes are projected to produce a different set of environmental conditions in the Tsoo-Yess River basin by the 2040s. Warmer air and water temperatures are projected for every month. Total annual precipitation in the 2040s is expected to be similar to the historical conditions, but the timing of precipitation should be different, with more precipitation in the winter and less in the summer. As surface water flows in the basin are driven by rainfall, changes in the timing of precipitation will lead to altered flow regimes with higher winter flows, with the potential for larger floods, and lower summer baseflows with more frequent and intense droughts.

Larger floods projected for the 2040s may pose an increased risk of damage to hatchery infrastructure. While Makah NFH is located within 4.8 km of the coast, continual flooding due to SLR is not predicted to be a major concern for the facility before 2050. Vertical land movement in that portion of the Olympic Peninsula, driven by subduction of the Juan de Fuca oceanic plate under the North American continental plate as well as isostatic rebound, is predicted to outpace global SLR through the 2050's under the majority of SLR models. However, increased coastal flooding during winter storms, including storm surges up the Tsoo-

Yess River, will be a concern for the facility and could lead to local flooding of low lying areas and saltwater intrusion into freshwater aquifers.

Warmer water throughout the year coupled with lower water availability in summer may not pose fundamental constraints on the propagation of Chinook salmon at Makah NFH, but these changes should result in a higher probability that coho salmon and steelhead reared under current practices will face increased physiological stress with a higher probability of disease and mortality. The Tsoo-Yess River is not a pathogen-free water source, and salmon reared at Makah NFH have already experienced significant outbreaks of disease, suggesting that health of coho salmon and steelhead in coming decades will be an increasingly significant concern.

Chinook salmon broodstock are collected during September to November, and juveniles are reared from October until release the following May. Predicted changes to climatic conditions in the Tsoo-Yess river basin during those months are less likely to seriously constrain the Chinook salmon program compared to the coho salmon and steelhead programs which include summer rearing. Nonetheless, some specific areas of concern for Chinook salmon may need to be addressed. Increased water temperatures will most likely affect the holding of Chinook salmon broodstock in September and October, potentially inducing physiological stress in adult fish. While increased temperatures during the rearing cycle are not predicted to exceed any physiological thresholds for juvenile Chinook, this warming will increase fish growth rates across the rearing cycle leading to larger fish size at release under current protocols. Increases in fish size are also the likely cause of modeled density index values exceeding fish health guidelines at the end of the rearing cycle in May.

Combined increases in water temperatures and density index values may increase disease risks for all species, especially at the end of the rearing cycle in May. Makah NFH relies

exclusively on surface water from the Tsoo-Yess River for rearing because no pathogen-free water sources are currently available for fish culture. Coho salmon and steelhead at Makah NFH have experienced outbreaks of *Aeromonas salmonicida*, the causative agent of Furunculosis, and *Ichthyophthirius multifiliis*, the causative agent of Ich, and outbreaks of these pathogens and *Ichthyobodo* sp. may be an increasing concern during the lifecycle of Chinook salmon reared at Makah NFH.

By the 2040s, coho salmon and steelhead at Makah NFH will be exposed to higher water temperatures in all months of the culture cycle. Steelhead broodstock are collected during November to January, and water temperatures during these months are not predicted to exceed any physiological tolerances for adult steelhead. On the other hand, coho salmon broodstock are collected from September to November, and increased water temperatures in September and October are predicted to exceed physiological tolerances for adults at the time of spawning. Consequently, adult coho salmon, especially those that are collected early in the season and held during the warmer months, may experience chronic thermal stress caused by exposure to high water temperatures. This stress would be expected to decrease immune function and increase the potential for disease outbreaks among captive adults held for broodstock, potentially leading to increased adult mortality.

By the 2040s, warmer water should lead to increased growth of juvenile coho salmon and steelhead in every month, and temperatures in June through September are expected to exceed the physiological thresholds for both species, thus increasing the risk of disease outbreaks. Coho salmon and steelhead at Makah NFH currently face significant problems with disease outbreaks of *Aeromonas salmonicida* (Asal), the causative agent of Furunculosis, and *Ichthyophthirius multifiliis*, the causative agent of Ich, in years with warm water temperatures and/or low flows.

Outbreaks of these pathogens may be an increasing concern during the rearing of both species on station as predicted climate change will exacerbate the conditions that are conducive to disease. Future water temperature during June-October at Makah NFH, when coho salmon and juvenile steelhead are on station, are well within the disease outbreak temperatures for some or all of the common pathogens (Table B2). Historically, both salmonid species have been susceptible to Asal and Ich during summer (USFWS 2014, 2015a, 2015b). For many years, steelhead and coho salmon have been repeatedly treated with formalin and antibiotics to control disease outbreaks. While treatments have been successful in some years, they have not been successful in other years. For example, a prolonged drought in 2015, characterized by extremely low water availability and high water temperatures, motivated the repeated use of antibiotics and ultimately in a decision to (a) release two-thirds of the age 0+ coho salmon and one-third of the age 0+ steelhead in early August (8 months early) and (b) euthanize the remaining coho salmon (one-third of the year class) to ensure adequate water for the remaining fish (steelhead) on station and to provide sufficient attractant water for adult Chinook salmon returning to the hatchery. Standard hatchery practices stressful to fish (e.g., handling, marking/tagging, moving fish between rearing containers) are often scheduled during the summer months and can exacerbate the effects of thermal stress, further increasing the probability of disease. For example, fish at Makah NFH are usually moved among raceways in June, a month that is predicted by the model to have a large increase in water temperature that exceeds the physiological tolerances of both coho salmon and steelhead.

Projected increases in water temperatures will most likely result in increased growth rates and larger fish at the time of release for all species reared at Makah NFH under current culture protocols. Chinook salmon are projected to be 15-30% heavier and 5-9% longer in most months.

Similarly, steelhead are projected to be 30-40% heavier and 9-12% longer, and coho salmon are projected to be 30-42% heavier and 6-12% longer in most months. While flow index values for Chinook salmon will most likely not exceed the guideline value of 1.0, density index values are predicted to exceed the guideline value of 0.20 in the final month of rearing (May). On the other hand, both flow and density index values for steelhead are predicted to exceed fish health guidelines in August and September, and during the final four months of rearing (January through April). Similarly, flow index values for coho program are predicted to exceed guideline values in August, and the density index values are predicted to exceed guideline values in September and the last three months of the rearing cycle prior to release (February through April).

Flow and density indices generally integrate growth, water use and physical capacity, and roughly approximate "carrying capacity" for total biomass based on dissolved oxygen levels, removal of metabolic waste, and the ecological and physiological consequences of crowding (Wedemeyer 2001). Biological consequences of flow and density index values that exceed fish health guideline values include reduced growth and condition, chronic stress, decreased immune function, and higher risk of disease. At the Makah NFH, increases in flow and density index values combined with predicted increases of water temperature into the disease outbreak ranges for several pathogens suggest that disease risks at the facility may be unacceptable by the 2040s under current culture protocols.

Coinciding with the summer months when density index values are predicted to increase significantly, Makah NFH has historically contended with low base flows that have required operational changes including reuse of water. Those low base flows are particularly acute in drought years. Reuse of water has been achieved by pumping hatchery effluent into a serpentine

channel upstream of the facility. This effluent is then mixed with fresh surface water from the Tsoo-Yess River and re-supplied to raceways. As this water passes through each raceway and is then pumped back into the serpentine channel, water quality is reduced by oxygen use and metabolic waste accumulation. This reduced water quality would effectively increase the density and flow indices for fish in raceways subject to reuse, but no accepted method exists currently to model those confounded effects. Therefore, the modeled density and flow index values we present here probably underestimate substantially the biological *effective* index values for fish in raceway that receive reused water.

Additionally, increased fish growth could compromise the ability to meet size-at-release targets. Large body size of individual fish at seawater entry has been positively correlated with an increased proportion of precocially-mature salmon, particularly males (aka "jacks") within a population (Vøllestad et al. 2004; Koseki and Fleming 2007). In addition, when larger juvenile salmon from a hatchery are released into an environment that contains smaller, natural-origin salmon, the hatchery-origin fish can also pose an ecological risk to the natural-origin fish through predation (Hawkins and Tipping 1999; Namen and Sharpe 2012) and competition (Weber and Fausch 2003; Simpson et al. 2009), thus reducing the productivity of natural populations.

Mitigating the effects of climate change at Makah NFH

In the future, Makah NFH will likely have to contend with year-round increases in water temperature of its source water, decreased water availability during the summer months, increased fish growth, and more frequent disease outbreaks. While these factors will affect all programs at the facility, the overall impact to the Chinook salmon program is expected to be modest in comparison to the coho salmon and steelhead programs that already face significant

operational challenges, particularly during the summer months and early fall. Under current conditions, the coho salmon and steelhead programs already require multiple chemical and antibiotic treatments to control pathogens and prevent disease outbreaks and mortality. Our modeling exercise predicts that the environmental conditions (high temperature and low stream flow) and rearing conditions at the hatchery (flow and density index values that exceed fish health guidelines) that often result in disease outbreaks will be more frequent in the 2040s and span an additional two months when compared to the historical record. These latter outcomes could preclude the future summer rearing of coho salmon and steelhead at Makah NFH.

Mitigation of climate-related effects is theoretically possible at Makah NFH, but many of the possible approaches have obvious drawbacks and might require further study to determine their efficacy. Many of the effects of climate change to salmon and steelhead at Makah NFH are due to increased water temperatures that increase fish growth and the likelihood of disease outbreaks, so colder water for fish culture would be a critical mitigation measure. If colder groundwater is available to the facility, it could conceivably be used to slow fish growth, although the facility currently has no infrastructure to use groundwater for rearing, and it is unknown if sufficient groundwater is available for fish culture at the facility. Mechanical cooling of surface water from the Tsoo-Yess River by using chillers is theoretically possible, and similar approaches have been implemented in other salmon hatcheries in the Pacific Northwest. However, direct cooling by even 1 to 2°C of the large volume of water that is supplied to the entire hatchery for multiple months would be energy intensive and likely cost prohibitive. To decrease energy costs, chilled water could be used early in rearing to slow fish growth, though it is unknown if a sufficient decrease in fish size could be attained by this method. Growth modulation through reduced rations could be used, although ration levels would need to be

maintained at a level that provides enough nutrition to minimize fish health problems. A mixed strategy that combined water chilling and reduced rations could be tested. Operationally, the hatchery could attempt to further refine water reuse during periods of lower water availability. Currently, reused water is untreated prior to being resupplied to raceways which may exacerbate disease risks in the facility by decreasing water quality and concentrating pathogens. Finally, managers could avoid exceeding density index guidelines (i.e., levels that would be expected to put fish at risk of disease) by rearing fewer fish or allowing for fish to be apportioned among more raceways at lower densities if sufficient water is available. However, these latter strategies, by themselves, would not eliminate the risk of disease because they do not address warmer water temperatures.

Acknowledgments

We thank Jarrett Page, Marsha McGee, and the staff at the Makah NFH for providing data and comments during the modeling process. The Region 1 NFH Climate Change Planning Team of Bill Gale, Patty Crandell and Don Campton provided general guidance on the scope and content of this project, and also contributed useful comments on this report. Ingrid Tohver (University of Washington, Climate Impacts Group) provided flow modeling data for the Tsoo-Yess River basin. Victoria O'Byrne performed watershed delineation and generated maps for the Tsoo-Yess River watershed. Madeline Steele conducted GIS analyses to extract downscaled climate flux data for the watershed. Kyle Hanson and Doug Peterson were supported by the USFWS Abernathy Fish Technology Center.

References

Anderson, R. O., and S. J. Gutreuter. 1983. Length, weight, and associated structural indices. Pages 283-300 in L. A. Nielson and D. L. Johnson, editors. Fisheries techniques. American Fisheries Society, Bethesda, Maryland.

Becker, C.D., and R. G. Genoway. 1979. Evaluation of the critical thermal maximum for determining thermal tolerance of freshwater fish. Environmental Biology of Fishes 4:245-256.

Beitinger, T. L., W. A. Bennett, and R. W. McCauley. 2000. Temperature tolerances of North American freshwater fishes exposed to dynamic changes in temperature. Environmental Biology of Fishes 58:237-275.

Beitinger, T. L., and R. W. McCauley. 1990. Whole-animal physiological processes for the assessment of stress in fishes. Journal of Great Lakes Research 16:542-575.

Bisson, P. A., B. E. Rieman, C. Luce, P. F. Hessburg, D. C. Lee, J. L. Kershner, G. H. Reeves, and R. E. Gresswell. 2003. Fire and aquatic ecosystems of the western USA: current knowledge and key questions. Forest Ecology and Management 178(1-2):213-229.

Carey, M. P., B. L. Sanderson, T. A. Friesen, K. A. Barnas, and J. D. Olden. 2011. Smallmouth bass in the Pacific Northwest: a threat to native species; a benefit for anglers. Reviews in Fisheries Science 19:305-315.

Dumas, A., J. France, and D. P. Bureau. 2007. Evidence of three growth stanzas in rainbow trout (*Oncorhynchus mykiss*) across life stages and adaptation of the thermal-unit growth coefficient. Aquaculture 267(1-4):139-146.

Elliott, J. M. 1981. Some aspects of thermal stress on freshwater teleosts. Pages 209-245 in: A. D. Pickering, editor. Stress and Fish. Academic Press, New York, NY.

Fabry, V. J., B. A. Seibel, R. A. Feely, and J. C. Orr. 2008. Impacts of ocean acidification on marine fauna and ecosystem processes. ICES Journal of Marine Science 65:414-432.

Good, C., and coauthors. 2009. The impact of water exchange rate on the health and performance of rainbow trout *Oncorhynchus mykiss* in water recirculation aquaculture systems. Aquaculture 294(1–2):80-85.

Hamlet, A.F., E.P. Salathé, and P. Carrasco. 2010a. Statistical downscaling techniques for global climate model simulations of temperature and precipitation with application to water resources planning studies. Chapter 4 in Final Report for the Columbia Basin Climate Change Scenarios Project, Climate Impacts Group, Center for Science in the Earth System, Joint Institute for the Study of the Atmosphere and Ocean, University of Washington, Seattle.

Hamlet, A.F., P. Carrasco, J. Deems, M.M. Elsner, T. Kamstra, C. Lee, S-Y Lee, G. Mauger, E. P. Salathe, I. Tohver, and L. Whitely Binder. 2010b. Final Project Report for the Columbia Basin Climate Change Scenarios Project, http://www.hydro.washington.edu/2860/report/.

Hanson, K.C. and D.P. Peterson. 2014. Modeling the potential impacts of climate change on Pacific salmon culture programs: an example at Winthrop National Fish Hatchery. Environmental Management. DOI 10.1007/s00267-014-0302-2

Hawkins SW, Tipping JM (1999) Predation by juvenile hatchery salmonids on wild fall Chinook salmon fry in the Lewis River, Washington. Calif. Fish Game 85:124–129

Huppert, D. D., A. Moore, and K. Dyson. 2009. Impacts of climate change on the coasts of Washington State. Pages 285-309 in J. S. Littell, M. McGuire Elsner, L. C. Whitely

Binder, and A.K. Snover, editors. The Washington Climate Change Impacts Assessment: Evaluating Washington's Future in a Changing Climate. Climate Impacts Group, University of Washington, Seattle.

Intergovernmental Panel on Climate Change (IPCC). 2000. Special report on emissions scenarios: a special report of working group III of the intergovernmental panel on climate change. Cambridge University Press, Cambridge, 600 pp.

IPCC. 2007. Climate change 2007: synthesis report. Intergovernmental Panel on Climate Change, Geneva, Switzerland.

IPCC. 2014. Climate Change 2014: Synthesis Report. Contribution of Working Groups I, II and III to the Fifth Assessment Report of the Intergovernmental Panel on Climate Change, Core Writing Team: R.K. Pachauri and L.A. Meyer (eds.), Geneva, Switzerland, 151 pp.

Isaak, D. J., C. H. Luce, B. E. Rieman, D. E. Nagel, E. E. Peterson, D. L. Horan, S. Parkes, and G. L. Chandler. 2010. Effects of climate change and wildfire on stream temperatures and salmonid thermal habitat in a mountain river network. Ecological Applications 20:1350-1371.

Iwama G.K. and A.F. Tautz. 1981. A simple growth model for salmonids in hatcheries. Canadian Journal of Fisheries and Aquatic Science 38:649-656.

Jobling, M. 2010. Are compensatory growth and catch-up growth two sides of the same coin? Aquaculture International 18(4):501-510.

Koseki, Y., and I. A. Fleming. 2007. Large-scale frequency dynamics of alternative male phenotypes in natural populations of coho salmon (*Oncorhynchus kisutch*): patterns, processes, and implications. Canadian Journal of Fisheries and Aquatic Sciences 64:743–753.

Liang, X., D. P. Lettenmaier, E. F. Wood, and S. J. Burges. 1994. A simple hydrologically based model of land-surface water and energy fluxes for general-circulation models. Journal of Geophysical Research 99(D7):14,415-14,428.

Luttershmidt, W. I., and V. H. Hutchinson. 1997. The critical thermal maximum: history and critique. Canadian Journal of Zoology 75:1561-1574.

Mantua, N., I. Tohver, and A. Hamlet. 2010. Climate change impacts on streamflow extremes and summertime stream temperature and their possible consequences for freshwater salmon habitat in Washington State. Climatic Change 102:187-223.

Mohseni, O., H. G. Stefan, and T. R. Erickson. 1998. A nonlinear regression model for weekly stream temperatures. Water Resource Research 34:2685–2692.

Moore, S.K., N.J. Mantua, and E.P. Salathe Jr, E. P. 2011. Past trends and future scenarios for environmental conditions favoring the accumulation of paralytic shellfish toxins in Puget Sound shellfish. Harmful Algae 10(5): 521–529.

Mote P, Petersen A, Reeder S, Shipman H, and Whitely-Binder L (2008) Sea level rise in the coastal waters of Washington State. A report by the University of Washington Climate Impacts Group and the Washington Department of Oceanography.

Namen, S. W., C. S. Sharpe (2012) Predation by hatchery yearling salmonids on wild subyearling salmonids in the freshwater environment: A review of studies, two case histories, and implications for management. Environmental Biology of Fishes 94:21-28.

Nash, J.E., and J.V. Sutcliffe. 1970. River flow forecasting through conceptual models. Journal of Hydrology 10:282-290.

NRC, 2012. Sea-level rise for the coasts of California, Oregon, and Washington: Past, present, and future. National Research Council, The National Academies Press, 32 pp.

Paladino, R. V., J. R. Spotila, J. P. Schubauer and K. T. Kowalski. 1980. The critical thermal maximum: a technique used to elucidate physiological stress and adaptation in fishes. Rev. Canad. Biol. 39: 115-122.

Petersen, J. H., and J. F. Kitchell. 2001. Climate regimes and water temperature changes in the Columbia River: bioenergetic implications for predators of juvenile salmon. Canadian Journal of Fisheries and Aquatic Sciences 58:1831–1841.

Piper, R.G., I.B. McElwain, L.E. Orme, J.P. McCraren, L.G. Fowler, and J.R. Leonard. 1982. Fish hatchery management. US Fish and Wildlife Service, Washington, D.C.

R Core Team. 2015. R: A language and environment for statistical computing. R Foundation for Statistical Computing, Vienna, Austria. URL http://www.R-project.org/.

Rahel, F. J., and J. D. Olden. 2008. Assessing the effects of climate change on aquatic invasive species Conservation Biology 22(3):521-533.

Scheuerell, M. D., and J. G. Williams. 2005. Forecasting climate-induced changes in the survival of Snake River spring/summer Chinook salmon (*Oncorhynchus tshawytscha*). Fisheries Oceanography 14(6):448-457.

Simpson WG, Kennedy BM, Ostrand KG (2009) Seasonal foraging and piscivory by sympatric wild and hatchery-reared steelhead from an integrated hatchery program. Environmental Biology of Fishes 86:473-482.

Snover AK, Whitely Binder L, Lopez J, Willmott E, Kay J, Howell D, Simmonds J (2007) Preparing for climate change: A guidebook for local, regional, and state governments. In association with and published by ICLEI- Local Governments for Sustainability, Oakland, CA.

US Fish and Wildlife Service (USFWS). 2014. Makah NFH – Past, present and future: a call for changes to ensure sustainability. Unpublished white paper, dated November 19, 2014. 4 pp.

USFWS. 2015a. Position Resource File – Project Leader at Makah National Fish Hatchery. Unpublished document, dated May 7, 2015. 16 pp.

USFWS 2015b. Position Resource file – Assistant Project Leader at Makah National Fish Hatchery. Unpublished document, dated May 7, 2015. 14 pp.

van Vuuren, D. P., and coauthors. 2011. The representative concentration pathways: an overview. Climatic Change 109(1):5-31.

van Vuuren, D. P., and T. R. Carter. 2014. Climate and socio-economic scenarios for climate change research and assessment: reconciling the new with the old. Climatic Change 122(3):415–429.

Vøllestad, L. A., J. Peterson, and T. P. Quinn. 2004. Effects of freshwater and marine growth rates on early maturity in male coho and Chinook salmon. Transactions of the American Fisheries Society 133:495-503.

Weber ED, Fausch KD (2003) Interactions between hatchery and wild salmonids in streams: differences in biology and evidence for competition. Can. J. Fish. Aquat. Sci. 60:1018–1036

Wedemeyer, G.A., editor. 2001. Fish hatchery management, second edition. American Fisheries Society, Bethesda, MD.

Wenger, S. J., D. J. Isaak, J. B. Dunham, K. D. Fausch, C. H. Luce, H. M. Neville, B. E. Rieman, M. K. Young, D. E. Nagel, D. L. Horan, and G. L. Chandler. 2011. Role of climate and invasive species in structuring trout distributions in the interior Columbia River Basin, USA. Canadian Journal of Fisheries and Aquatic Sciences 68(6):988–1008.

Westerling, A.L., H.G. Hidalgo, D.R. Cayan, and T.W. Swetnam. 2006. Warming and earlier spring increases Western U.S. forest wildfire activity. Science 313: 940-943. DOI:10.1126/science.1128834

Table B1. Thermal tolerances (°C) of species reared at Makah NFH.

Species	Latin Binomial	Life-History Stage	Optimal Temp. Range	Optimal Temp. Growth Range	Spawn Range	Smoltification Threshold
Chinook Salmon	*O. tshawytscha*	adult	6.0 – 14.0 °C		9.0 – 12.3 °C	
		egg/fry	8.4 – 12.4 °C			
		juvenile	8.6 – 15.9 °C	14.0 – 18.4 °C		14.0 °C
Steelhead trout	*O. mykiss*	adult			6.4 – 15.3° C	
		egg/fry	7.4 – 14.0° C			
		juvenile	13.1 – 17.2° C	11.2 – 18.0° C		12.6° C
Coho salmon	*O. kisutch*	adult			5.7 – 11.7° C	
		egg/fry	1.7 – 9.9° C			
		juvenile	7.4 – 15.6° C	16.5 – 17.0° C[1]		14.3° C

[1]The optimal growth temperature range for juvenile coho salmon was obtained from only two available literature sources.

Table B2. Thermal range (°C) at which common salmon pathogens cause disease in Pacific salmon and steelhead.

Disease Name	Pathogen Name (causative agent)	Disease Outbreak Temperatures	Minimum Disease Temperatures
Bacteria diseases			
Furunculosis	*Aeromonas salmonicida (A.sal)*	20.0 – 22.0 °C	12.0 °C
Vibriosis	*Vibrio anguillarum*	18.0 – 20.0 °C	14.0 °C
Enteric redmouth disease	*Yersinia ruckeri*	22.0 °C	11.0 – 18.0 °C
Columnaris disease	*Flavobacterium columnaris*	28.0 – 30.0 °C	15.0 °C
Coldwater disease (fin rot)	*Flavobacterium psychrophilum*	4.0 – 10.0 °C	4.0 – 10.0 °C
Bacterial kidney disease	*Renibacterium salmoninarum*		15.0 °C
Fungal diseases			
Saprolegniasis	*Saprolegnia parasitica, Achyla hoferi, Dictyuchus* spp.	15.0 – 30.0 °C	
Parasitic diseases			
Parasitic ichtyobodiasis (Costiasis)	*Ichthyobodo necatrix, I. pyrifornis*	10.0 – 25.0 °C	
White spot disease (Ich)	*Ichthyophthirius multifiliis*	24.0 – 26.0 °C	12.0 – 15.0 °C
Proliferative kidney disease	*Tetracapsuloides bryosalmonae*	16.0 °C	
Ceratomyxosis	*Ceratonova shasta*	15.0 – 25.0 °C	10.0 – 15.0 °C
Viral diseases			
Infectious pancreatic necrosis virus (IPNV) disease	*Aquabirnavirus* sp.	20.0 – 23.0 °C	
Infectious hematopoietic necrosis (IHN) disease	*Novirhadovirus* sp.	13.0 – 18.0 °C	15.0 °C

Table B3. Mean monthly water temperatures of sources that supply Makah NFH. Historical values for Tsoo-Yess River are empirical data (ºC ± S.D.) from 8-year historical baseline (1982 – 1989). Predictions for the 2040s were calculated by adding the monthly difference between modeled historical and future water temperatures to the empirical historical baseline. Modeled future values for surface water temperatures were derived from statistically downscaled air temperatures from 10 global circulation models under the A1B emissions scenario and regression relationships between air and surface waters (see text for additional details).

Month	**Historical baseline (ºC ± S.D.)**	**2040s A1B (ºC ± S.D.) Predicted (Min. – Max.)**
January	5.9 ± 0.4	6.9 (6.1 – 7.5)
February	5.9 ± 0.7	7.2 (6.1 – 8.2)
March	7.7 ± 0.4	8.7 (7.9 – 9.2)
April	9.9 ± 0.8	11.4 (10.2 – 13.3)
May	12.8 ± 1.2	14.7 (13.9 – 17.1)
June	15.6 ± 0.6	17.7 (16.4 – 19.0)
July	17.2 ± 0.8	19.6 (18.7 – 21.2)
August	18.0 ± 0.5	20.4 (19.5–21.0)
September	15.2 ± 1.3	17.6 (16.7 – 18.9)
October	11.3 ± 1.3	13.3 (12.8 – 14.1)
November	8.0 ± 1.2	9.3 (8.9 – 9.8)
December	5.5 ± 0.8	6.6 (5.9 – 7.4)

Table B4. Modeled historical and future monthly average air temperatures (T_{ave}), precipitation, and snow water equivalent (SWE) for the area of overlap between the 1/16° grid cells and the watershed boundary of Makah NFH. Modeled projected future values are ensemble means based on 10 global climate models (GCM) extracted from monthly flux files and based on the A1B climate scenario; and SD represents the variability in monthly estimates among the 10 GCM. An example of the url location for a monthly flux file for one of the GCMs is: http://warm.atmos.washington.edu/2860/r7climate/hb2860_hybrid_delta_runs/echam5_A1B_2030-2059/fluxes_monthly_summary/.

Month	T_{ave} (°C) Historical	T_{ave} (°C) Projected 2040s (± S.D.)	T_{ave} (°C) Diff.	PPT (mm) Historical	PPT (mm) Projected 2040s (± S.D.)	PPT (mm) Diff.	SWE (mm) Historical	SWE (mm) Projected 2040s (± S.D.)	SWE (mm) Diff.
January	3.5	4.9 ± 0.87	1.4	426	458 ± 45	32	1.6	0.5 ± 0.4	-1.1
February	6.7	8.1 ± 0.85	1.4	335	349 ± 51	14	7.9	9.4 ± 7.8	1.5
March	5.7	7.0 ± 0.63	1.3	309	335 ± 19	26	0.4	1.3 ± 3.7	0.9
April	7.9	9.4 ± 0.75	1.5	207	217 ± 28	10	0.0	0.1 ± 0.4	0.1
May	10.8	12.4 ± 0.81	1.6	122	115 ± 13	-7	0.0	0.0 ± 0.0	–
June	13.4	15.1 ± 0.65	1.8	87	71 ± 17	-16	0.0	0.0 ± 0.0	–
July	15.0	17.4 ± 0.82	2.4	58	40 ± 12	-18	0.0	0.0 ± 0.0	–
August	15.2	17.6 ± 0.47	2.4	64	51 ± 15	-13	0.0	0.0 ± 0.0	–
September	13.9	16.1 ± 0.64	2.2	125	113 ± 25	-12	0.0	0.0 ± 0.0	–
October	10.6	12.4 ± 0.34	1.8	304	343 ± 33	39	0.0	0.0 ± 0.0	–
November	6.6	8.1 ± 0.35	1.5	416	475 ± 65	58	0.0	0.0 ± 0.0	–
December	4.6	6.2 ± 0.57	1.6	468	506 ± 33	37	0.4	0.2	-0.2

Table B5. Projected mean annual flows (cfs) in the 2040s in the Tsoo-Yess River based on VIC hydrologic model forced by output from 10 global circulation models (GCM) under the A1B emissions scenario. For comparison, the modeled historical flow was 454 cfs.

GCM	Mean annual flow in 2040s (cfs)
ccsm3	429
cgcm3	522
cnrm_cm3	475
echam5	479
echo_g	457
Hadcm	474
hadgem1	424
ipsl_cm4	509
miroc_3.2	535
pcm1	445
2040s ensemble AVERAGE	485

Table B6. Mean monthly water temperatures experienced by adult broodstock and earlier life history stages of Chinook salmon reared at Makah NFH based on the historical baseline (1982 – 1989) and projected values for the 2040's.

Month	Life History Stage	Historical baseline water temperature (°C)	A1B projected 2040s water temperature (°C)
September	Broodstock	15.2	17.6
October	Broodstock	11.3	13.3
November	Broodstock	8.0	9.3
October	egg/fry	11.3	13.3
November	egg/fry	8.0	9.3
December	egg/fry	5.5	6.6
January	egg/fry	5.9	6.9
February	juvenile	5.9	7.2
March	juvenile	7.7	8.7
April	juvenile	9.9	11.4
May	smolt	12.8	14.7

Table B7. Monthly size differences of juvenile Chinook salmon reared at Makah NFH exposed to projected water temperatures for the 2040s relative to fish reared at water temperatures from the historical baseline (1982 – 1989).

Month	Life-History Stage	Weight (g) difference	Length (mm) difference
January	egg/fry	8.6%	2.8%
February	juvenile	16.0%	5.0%
March	juvenile	20.4%	6.3%
April	juvenile	25.1%	7.7%
May	smolt	29.4%	8.9%

Table B8. Modeled flow and density index values and constituent variables for Chinook salmon at Makah NFH. Rearing parameters (Rear.) are based on hatchery averages for brood years 2010-2014. Historical (Hist.) and bias-adjusted future (2040s) flow and density indexes are shown graphically in Figure B12. For additional details, see Online Resource 2 at Hanson and Peterson (2014).

Time step (*i*)	Month[a]	Rear. N_i [b]	Rear. C_i(ft^3)[c]	Rear. d_i [d]	Hist. L_i [e]	Hist. W_i [f]	Hist. GPM_i[g]	Hist. DI_i [h]	Hist. FI_i [i]	2040s L_i [e]	2040s W_i [f]	2040s GPM_i[g]	2040s DI_i [h]	2040s FI_i[i]	r_i[j]
1	Jan	1,132,177	12,695	31	1.95	1.38	2,842	0.14	0.62	2.01	1.50	2,842	0.15	0.65	0.73
2	Feb	1,709,798	16,442	28	2.24	2.09	3,433	0.21	1.02	2.35	2.42	3,433	0.24	1.13	0.60
3	Mar	2,108,138	32,872	31	2.65	3.46	8,149	0.18	0.74	2.82	4.16	8,149	0.21	0.84	0.69
4	Apr	2,070,539	36,754	30	3.15	5.87	9,836	0.23	0.86	3.40	7.34	9,836	0.27	1.00	0.55
5	May	2,062,173	41,106	31	3.85	10.51	10,410	0.30	1.20	4.16	13.59	10,113	0.36	1.47	0.67

[a] Calendar month in rearing cycle. Numbers in parentheses indicate the year for that rearing cycle.

[b] Numbers of post-hatch juvenile fish or abundance (N_i) based on hatchery averages during 2010-2014 brood years.

[c] Mean hatchery capacity (C_i) used during 2007-2010 based on the number of raceways, their sizes, and water depth.

[d] Number of days (d_i) in the monthly time-step *i*.

[e] Modeled historical or projected future average fish length (L_i) in inches, at each monthly time-step *i*.

[f] Modeled historical or projected future average fish weight (W_i) in grams, at each monthly time-step *i*.

[g] Estimated mean historical or future projected flow rates through the hatchery (GPM_i) in gallons per minute at each monthly time-step *i*. Future projected flow rates are based on the expected changes in mean monthly discharge in the Tsoo-Yess River, with the assumption that the hatchery will not utilize any more water than the historical amount at any given time-step; thus only reductions in water availability are depicted.

[h] Modeled historical or projected future density index (DI_i) at time-step *i*.

[i] Modeled historical or projected future flow index (FI_i) at time-step *i*.

[j] Bias correction factors are the ratio between empirical mean index values and simulated historical values (see also footnote at bottom of page 16):

$$r_i = rFI_i = \frac{FI_i \text{ mean empirical historical}}{FI_i \text{ modeled historical}} = rDI_i = \frac{DI_i \text{ mean empirical historical}}{DI_i \text{ modeled historical}}$$

For additional details, see Online Resource 2 at Hanson and Peterson (2014).

Table B9. Mean monthly water temperatures experienced by adult broodstock and earlier life history stages of coho salmon reared at Makah NFH based on the historical baseline (1982 – 1989) and projected values for the 2040's.

Month	Life History Stage	Historical baseline water temperature (°C)	A1B projected 2040s water temperature (°C)
September	Broodstock	15.2	17.6
October	Broodstock	11.3	13.3
November	Broodstock	8.0	9.3
December	egg/fry	5.5	6.6
January	egg/fry	5.9	6.9
February	egg/fry	5.9	7.2
March	juvenile	7.7	8.7
April	juvenile	9.9	11.4
May	juvenile	12.8	14.7
June	juvenile	15.7	17.7
July	juvenile	17.2	19.6
August	juvenile	18.1	20.5
September	juvenile	15.2	17.6
October	juvenile	11.3	13.3
November	juvenile	8.0	9.3
December	juvenile	5.5	6.6
January	juvenile	5.9	6.9
February	juvenile	5.9	7.2
March	juvenile	7.7	8.7
April	smolt	9.9	11.4

Table B10. Monthly size differences of juvenile coho salmon reared at Makah NFH exposed to projected water temperatures for the 2040s relative to fish reared at water temperatures from the historical baseline (1982 – 1989).

Month	Life-History Stage	Weight (g) difference	Length (mm) difference
February (1)	egg/fry	10.2%	3.3%
March (1)	Juvenile	16.4%	5.2%
April (1)	Juvenile	22.5%	6.9%
May (1)	Juvenile	27.8%	8.4%
June (1)	Juvenile	30.7%	9.2%
July (1)	Juvenile	33.3%	10.0%
August (2)	Juvenile	34.9%	10.4%
September (2)	Juvenile	36.9%	10.9%
October (2)	Juvenile	38.7%	11.4%
November (2)	Juvenile	39.1%	11.5%
December (2)	Juvenile	39.8%	11.7%
January (2)	Juvenile	40.1%	11.8%
February (2)	Juvenile	40.8%	12.0%
March (2)	Juvenile	40.7%	11.9%
April (2)	Smolt	40.9%	12.0%

Table B11. Modeled flow and density index values and constituent variables for coho salmon at Makah NFH. Rearing parameters (Rear.) are based on hatchery averages for brood years 2010-2013. Historical (Hist.) and bias-adjusted future (2040s) flow and density indexes are shown graphically in Figure B16. For additional details, see Online Resource 2 at Hanson and Peterson (2014).

Time step (*i*)	Month[a]	Rear. N_i [b]	Rear. C_i(ft^3)[c]	Rear. d_i [d]	Hist. L_i [e]	Hist. W_i [f]	Hist. GPM_i[g]	Hist. DI_i [h]	Hist. FI_i [i]	2040s L_i [e]	2040s W_i [f]	2040s GPM_i[g]	2040s DI_i [h]	2040s FI_i[i]	r_i[j]
1	Feb	167,059	2,418	28	1.82	1.1	434	0.09	0.52	1.88	1.2	434	0.10	0.56	0.69
2	Mar	211,606	4,030	31	2.24	2.1	587	0.11	0.74	2.35	2.4	587	0.12	0.82	0.77
3	Apr	300,853	4,836	30	2.75	3.9	1,134	0.19	0.82	2.94	4.7	1,134	0.22	0.94	0.66
4	May	292,694	5,642	31	3.42	7.5	1,459	0.25	0.97	3.71	9.6	1,417	0.30	1.18	0.61
5	Jun	278,864	7,254	30	4.21	14.1	1,931	0.28	1.07	4.60	18.4	1,681	0.34	1.47	0.41
6	Jul	276,029	7,254	31	5.10	25.1	1,759	0.41	1.71	5.60	33.5	1,441	0.50	2.53	0.31
7	Aug	274,826	7,254	31	6.01	41.3	1,660	0.57	2.51	6.63	55.8	1,301	0.70	3.92	0.26
8	Sep	274,033	7,254	30	6.72	58.0	1,845	0.72	2.83	7.45	79.4	1,489	0.89	4.32	0.23
9	Oct	263,216	12,090	31	7.23	72.5	3,229	0.48	1.80	8.05	100.5	3,229	0.60	2.24	0.23
10	Nov	261,925	15,314	30	7.54	82.4	4,035	0.41	1.56	8.41	114.6	4,035	0.51	1.95	0.26
11	Dec	261,931	15,314	31	7.72	88.6	3,814	0.43	1.74	8.63	123.8	3,814	0.54	2.17	0.28
12	Jan	240,875	15,113	31	7.92	95.8	3,594	0.42	1.79	8.86	134.2	3,594	0.53	2.24	0.34
13	Feb	229,351	14,508	28	8.09	102.0	3,298	0.44	1.93	9.06	143.6	3,298	0.55	2.43	0.38
14	Mar	208,652	13,904	31	8.38	113.3	3,011	0.45	2.07	9.37	159.3	3,011	0.56	2.60	0.37
15	Apr	208,574	13,904	30	8.76	129.6	3,011	0.49	2.26	9.80	182.5	3,011	0.62	2.84	0.34

[a] Calendar month in rearing cycle.

[b] Numbers of post-hatch juvenile fish or abundance (N_i) based on hatchery averages during 2010-2013 brood years.

[c] Mean hatchery capacity (C_i) during 2010-2013 based on the number of raceways, their sizes, and water depth.

[d] Number of days (d_i) in the monthly time-step *i*.

[e] Modeled historical or projected future average fish length (L_i) in inches, at each monthly time-step *i*.

[f] Modeled historical or projected future average fish weight (W_i) in grams, at each monthly time-step *i*.

[g] Estimated mean historical or future projected flow rates through the hatchery (GPM_i) in gallons per minute (gpm) at each monthly time-step *i*. Future projected flow rates are based on the expected changes in mean monthly discharge in the Tsoo-Yess River, with the assumption that the hatchery will not utilize any more water than the historical amount at any given time-step; thus only reductions in water availability are depicted.

[h] Modeled historical or projected future density index (DI_i) at time-step *i*.

[i] Modeled historical or projected future flow index (FI_i) at time-step *i*.

[j] Bias correction factors are the ratio between empirical mean index values and simulated historical values (see also footnote at bottom of page 16):

$$r_i = rFI_i = \frac{FI_i \text{ mean empirical historical}}{FI_i \text{ modeled historical}} = rDI_i = \frac{DI_i \text{ mean empirical historical}}{DI_i \text{ modeled historical}}$$

For additional details, see Online Resource 2 at Hanson and Peterson (2014).

Table B12. Mean monthly water temperatures experienced by adult broodstock and earlier life stages of steelhead reared at Makah NFH based on the historical baseline (1982 – 1989) and projected values for the 2040's.

Month	Life History Stage	Historical baseline water temperature (°C)	A1B projected 2040s water temperature (°C)
November	Broodstock	8.0	9.3
December	Broodstock	5.5	6.6
January	Broodstock	5.9	6.9
January	egg/fry	5.9	6.9
February	egg/fry	5.9	7.2
March	egg/fry	7.7	8.7
April	juvenile	9.9	11.4
May	juvenile	12.8	14.7
June	juvenile	15.7	17.7
July	juvenile	17.2	19.6
August	juvenile	18.1	20.5
September	juvenile	15.2	17.6
October	juvenile	11.3	13.3
November	juvenile	8.0	9.3
December	juvenile	5.5	6.6
January	juvenile	5.9	6.9
February	juvenile	5.9	7.2
March	juvenile	7.7	8.7
April	smolt	9.9	11.4

Table B13. Monthly size differences of juvenile steelhead reared at Makah NFH exposed to projected water temperatures for the 2040s relative to fish reared at water temperatures from the historical baseline (1982 – 1989).

Month	Life-History Stage	Weight (g) difference	Length (mm) difference
March (1)	egg/fry	11.9%	3.8%
April (1)	Juvenile	21.3%	6.6%
May (1)	Juvenile	28.4%	8.6%
June (1)	Juvenile	31.8%	9.5%
July (1)	Juvenile	34.7%	10.3%
August (2)	Juvenile	36.3%	10.8%
September (2)	Juvenile	38.4%	11.3%
October (2)	Juvenile	40.2%	11.8%
November (2)	Juvenile	40.6%	11.9%
December (2)	Juvenile	41.3%	12.1%
January (2)	Juvenile	41.6%	12.2%
February (2)	Juvenile	42.4%	12.4%
March (2)	Juvenile	42.1%	12.3%
April (2)	Smolt	42.2%	12.3%

Table B14. Modeled flow and density index values and constituent variables for steelhead at Makah NFH. Rearing parameters (Rear.) are based on hatchery averages for brood years 2011-2014. Historical (Hist.) and bias-adjusted future (2040s) flow and density indexes are shown graphically in Figure B20. For additional details, see Online Resource 2 at Hanson and Peterson (2014).

Time step (*i*)	Month[a]	Rear. N_i [b]	Rear. C_i(ft^3)[c]	Rear. d_i [d]	Hist. L_i [e]	Hist. W_i [f]	Hist. GPM_i[g]	Hist. DI_i [h]	Hist. FI_i [i]	2040s L_i [e]	2040s W_i [f]	2040s GPM_i[g]	2040s DI_i [h]	2040s FI_i[i]	r_i[j]
1	Mar	174,390	1,024	31	1.50	0.6	341	0.16	0.47	1.56	0.7	341	0.17	0.50	0.55
2	Apr	260,097	2,636	30	2.02	1.5	806	0.16	0.54	2.16	1.9	806	0.19	0.61	0.55
3	May	251,193	4,836	31	2.71	3.7	1,211	0.16	0.63	2.94	4.8	1,177	0.19	0.76	0.63
4	Jun	205,050	8,060	30	3.51	8.1	2,109	0.13	0.50	3.85	10.7	1,835	0.16	0.69	0.59
5	Jul	203,467	8,060	31	4.41	16.2	1,987	0.20	0.83	4.87	21.8	1,628	0.25	1.24	0.58
6	Aug	202,417	8,060	31	5.33	28.9	1,931	0.30	1.25	5.91	39.3	1,514	0.37	1.96	0.57
7	Sep	198,004	8,060	30	6.06	42.5	2,184	0.38	1.40	6.74	58.8	1,763	0.47	2.16	0.52
8	Oct	163,817	12,090	31	6.59	54.7	5,111	0.25	0.59	7.36	76.7	5,111	0.31	0.74	0.51
9	Nov	163,431	12,896	30	6.91	63.4	5,263	0.26	0.63	7.74	89.1	5,263	0.32	0.79	0.53
10	Dec (1)	163,310	12,896	31	7.11	69.0	5,158	0.27	0.68	7.97	97.6	5,158	0.34	0.85	0.54
11	Jan (2)	153,747	12,695	31	7.33	75.6	4,640	0.28	0.75	8.22	107.0	4,640	0.35	0.95	0.59
12	Feb (2)	147,785	12,695	28	7.51	81.4	4,484	0.28	0.79	8.44	115.9	4,484	0.35	1.00	0.62
13	Mar (2)	147,549	12,695	31	7.81	91.6	4,559	0.30	0.84	8.77	130.2	4,559	0.38	1.06	0.63
14	Apr (2)	128,911	12,090	30	8.20	106.4	2,767	0.30	1.33	9.22	151.4	2,767	0.39	1.69	0.55

[a] Calendar month in rearing cycle.

[b] Numbers of post-hatch juvenile fish or abundance (N_i) based on hatchery averages during 2011-2014 brood years.

[c] Mean hatchery capacity (C_i) during 2011-2014 based on the number of raceways, their sizes, and water depth.

[d] Number of days (d_i) in the monthly time-step *i*.

[e] Modeled historical or projected future average fish length (L_i) in inches, at each monthly time-step *i*.

[f] Modeled historical or projected future average fish weight (W_i) in grams, at each monthly time-step *i*.

[g] Estimated mean historical or future projected flow rates through the hatchery (GPM_i) in gallons per minute (gpm) at each monthly time-step *i*. Future projected flow rates are based on the expected changes in mean monthly discharge in the Tsoo-Yess River, with the assumption that the hatchery will not utilize any more water than the historical amount at any given time-step; thus only reductions in water availability are depicted.

[h] Modeled historical or projected future density index (DI_i) at time-step *i*.

[i] Modeled historical or projected future flow index (FI_i) at time-step *i*.

[j] Bias correction factors are the ratio between empirical mean index values and simulated historical values (see also footnote at bottom of page 16):

$$r_i \;=\; rFI_i = \frac{FI_i \text{ mean empirical historical}}{FI_i \text{ modeled historical}} \;=\; rDI_i = \frac{DI_i \text{ mean empirical historical}}{DI_i \text{ modeled historical}}$$

For additional details, see Online Resource 2 at Hanson and Peterson (2014).

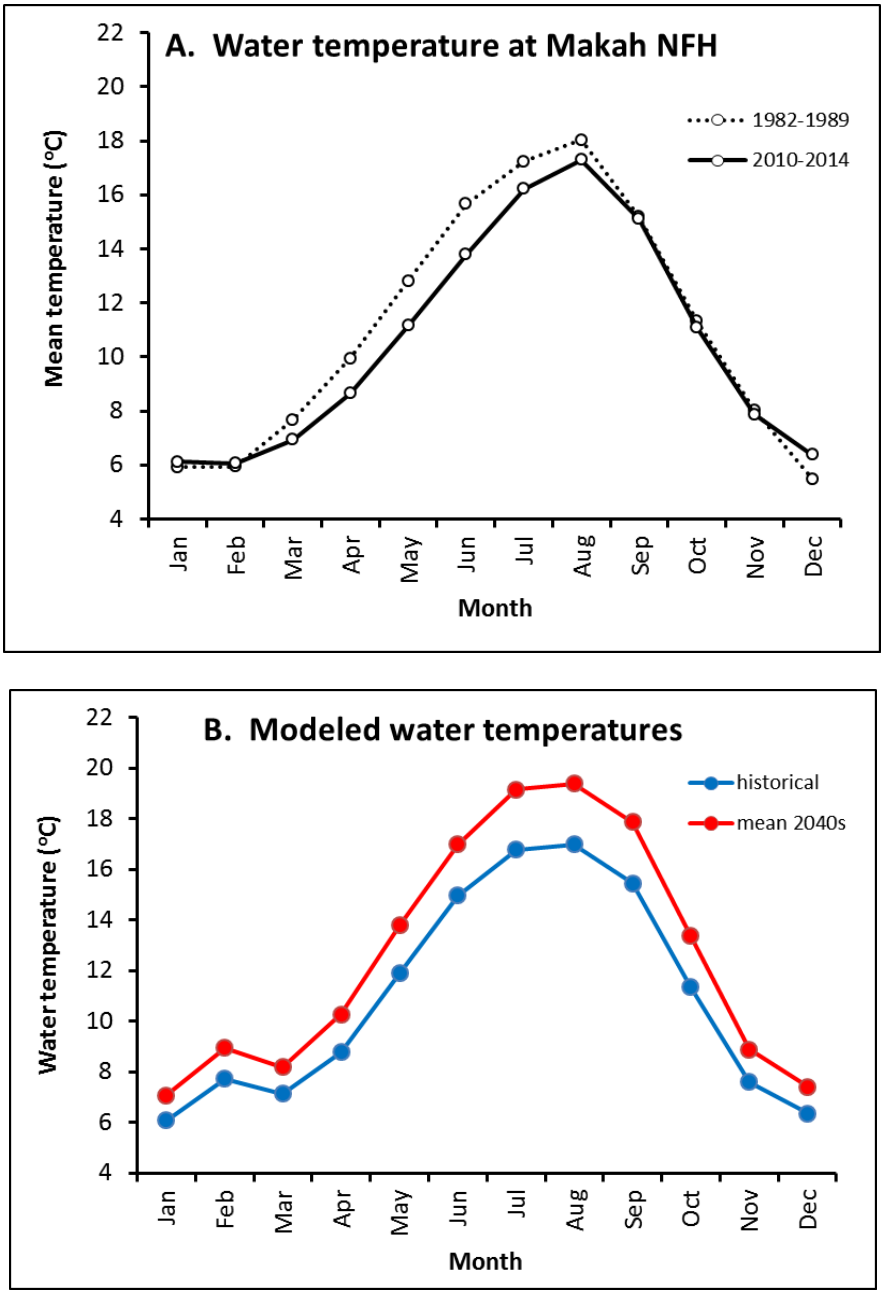

Figure B1. Empirical (panel A) and modeled (panel B) water temperatures for the Tsoo-Yess River near Makah NFH. Two time series of empirical data were available (panel A). The 1982-1989 data were used in the regression analyses and modeling of future water temperatures (panel B). In panel A, mean annual temperature was 11.1°C for1982-89 and 10.6°C for 2010-14. The historical and future modeled temperatures exhibited unexpected fluctuations in the Jan-Mar time period, rather than steady warming; this was apparently an artefact of the underlying climate flux files for that specific geographic location. Consequently, predicted values for the 2040s were calculated by incrementing the selected empirical historical values (dotted line, panel A) with the difference between the modeled historical and future values (panel B); these predictions are presented in Figure B2 and Table B3.

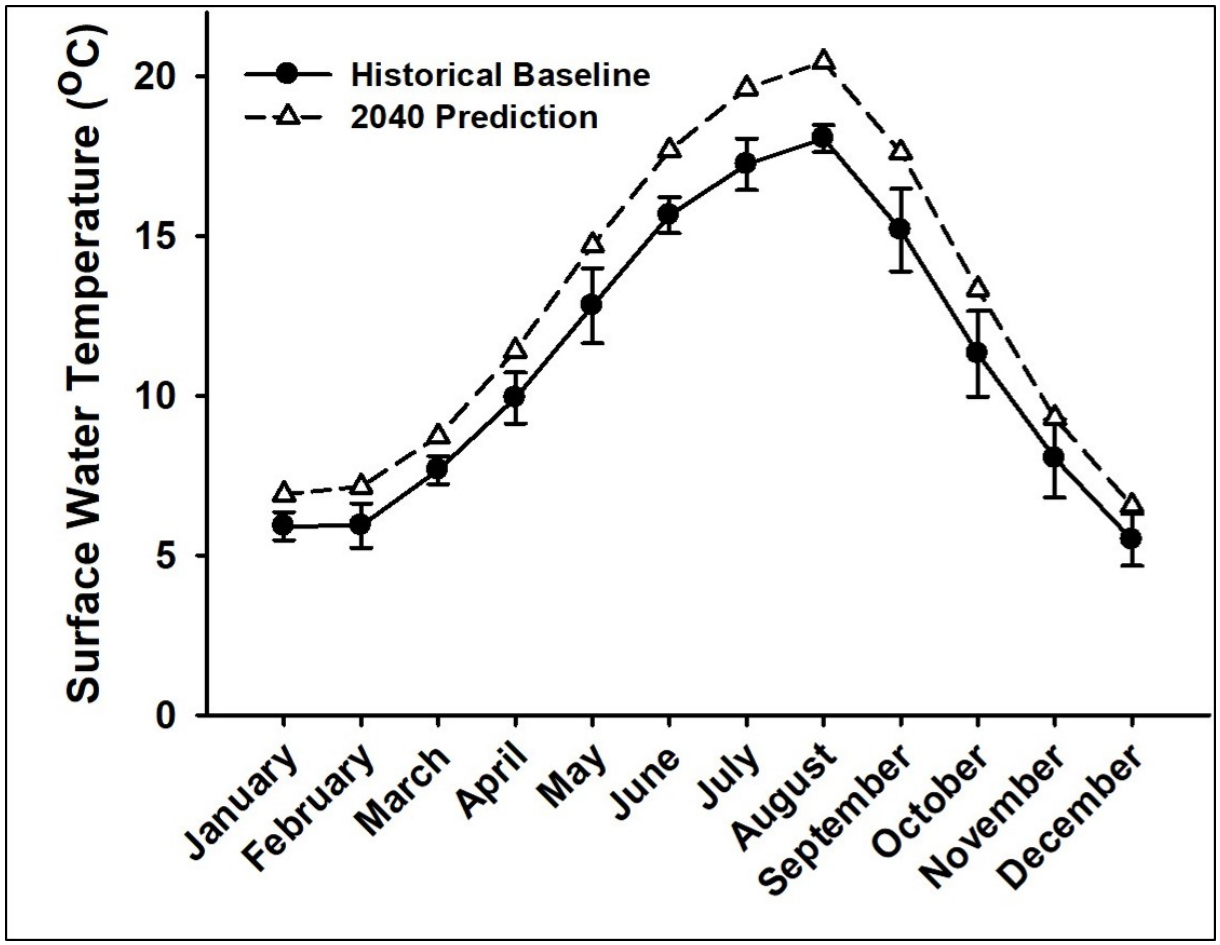

Figure B2. *Comparison of the mean (± S.D.) water temperatures of water source that supplies Makah NFH from the empirical historical baseline (1982 – 1989) and projected values for the 2040s. The projected values were calculated by incrementing the empirical baseline values by the difference in difference between the modeled historical and future temperatures presented in Figure B1, panel B. These data were subsequently used to model fish growth at Makah NFH.*

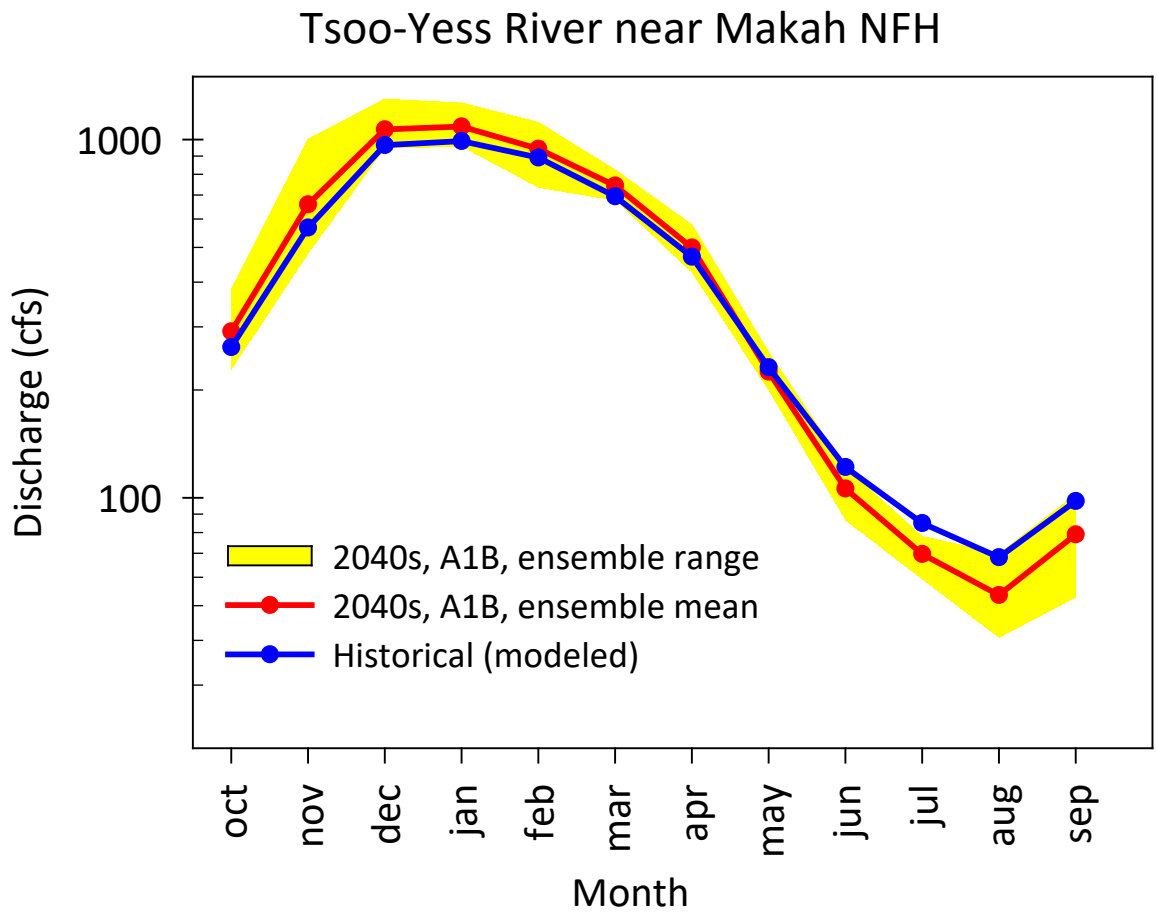

Figure B3. *Mean monthly surface flow in Tsoo-Yess River adjacent to the Makah National Fish Hatchery based on raw Variable Infiltration Capacity (VIC) simulations. Projected (2040s) surface flows are based on the VIC model forced by output from an ensemble of 10 general circulation models (GCM) under the A1B greenhouse gas emissions scenario.*

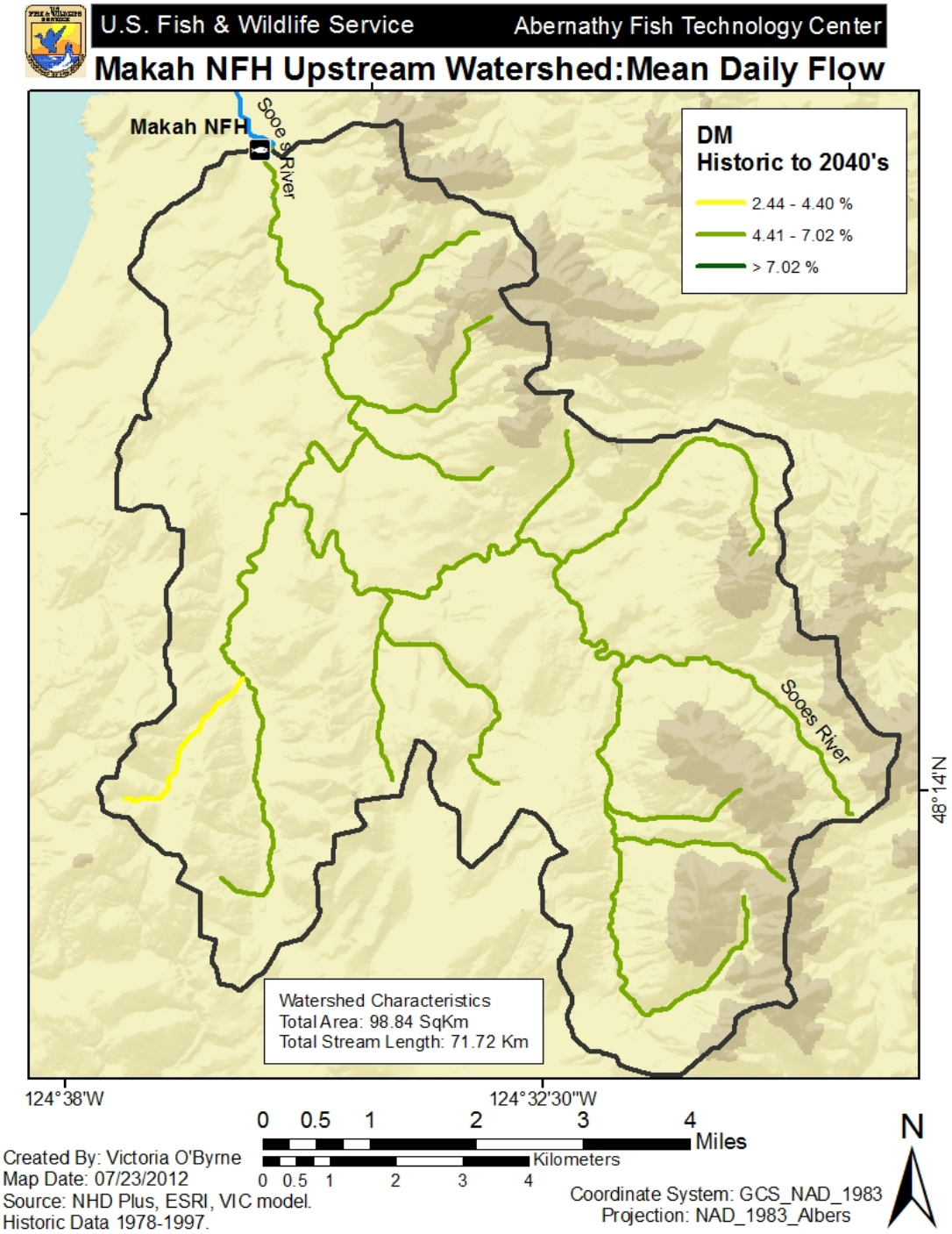

Figure B4. *Projected change mean daily flow (DM, in %) for the Tsoo-Yess River basin upstream from Makah NFH between historical and 2040s time periods. Data are from VIC hydrologic model (Wenger et al. 2011b) and the historical reference period is 1978-1997.*

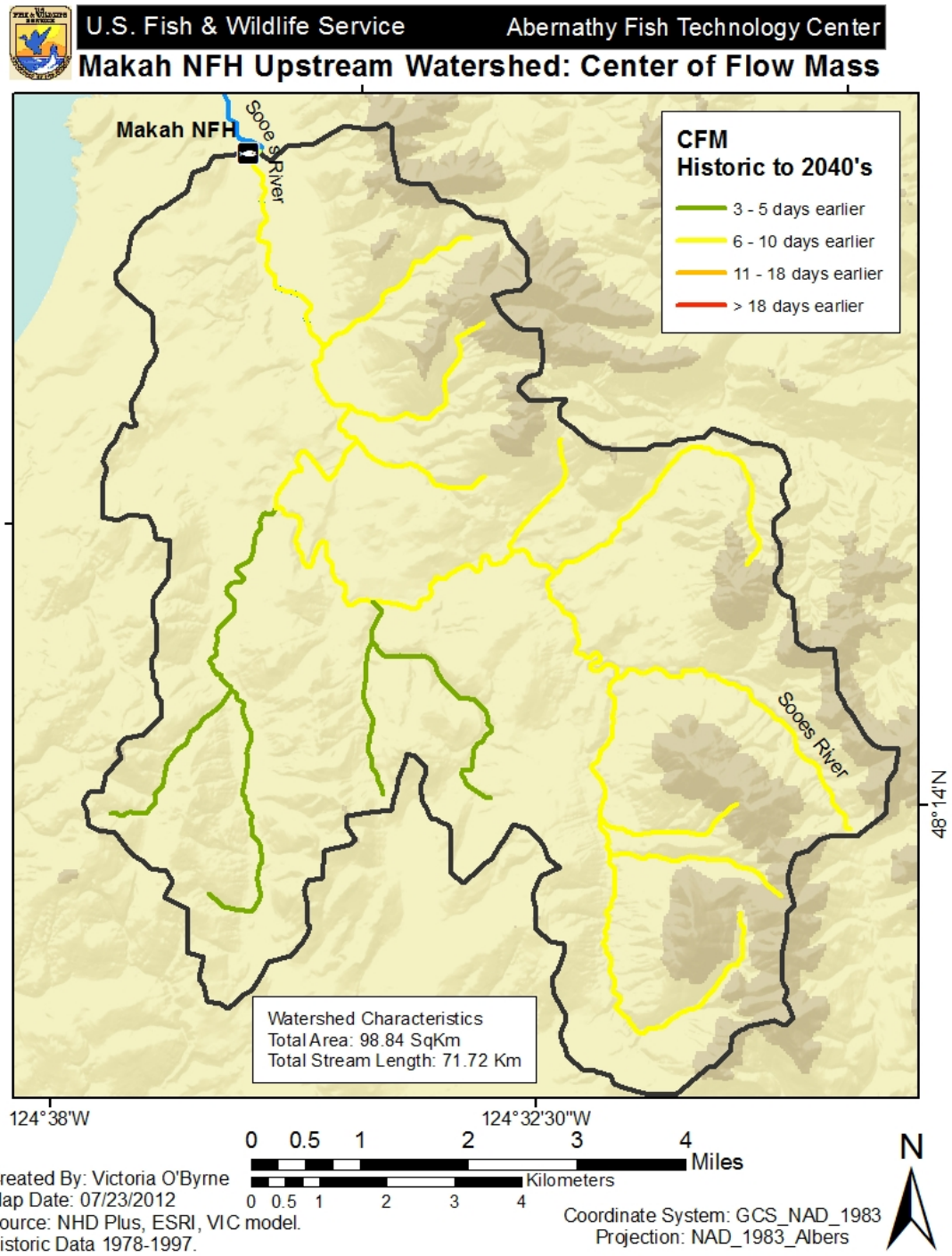

Figure B5. *Projected change in the timing of snowmelt runoff (date of center of flow mass, CFM) for the Tsoo-Yess River basin upstream from Makah NFH between historical and 2040s time periods. Data are from VIC hydrologic model (Wenger et al. 2011b) and the historical reference period is 1978-1997.*

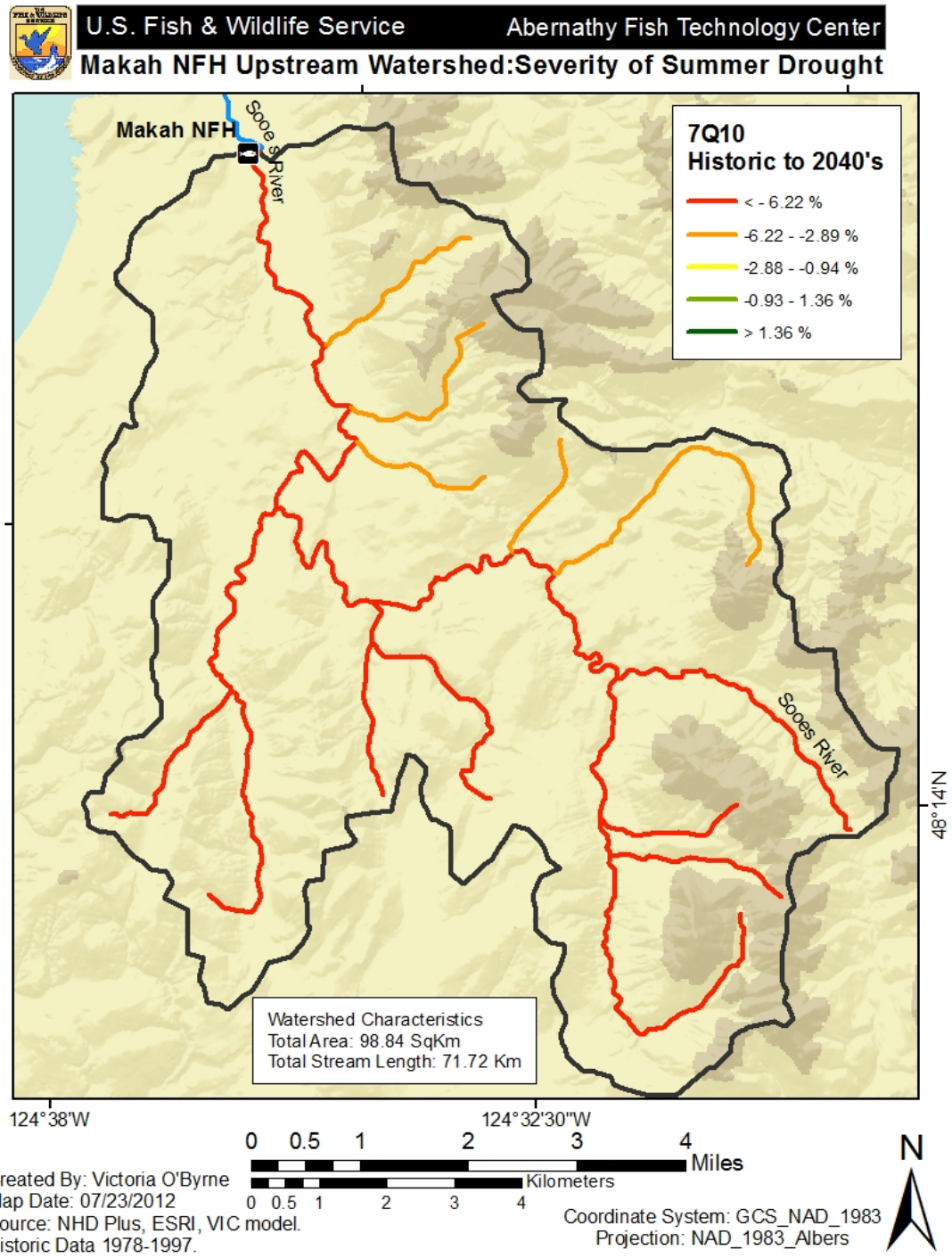

Figure B6. *Projected change in the severity of summer drought (7-day low flow 10-yr return interval, 7Q10) for the Tsoo-Yess River basin upstream from Makah NFH between historical and 2040s time periods. Data are from VIC hydrologic model (Wenger et al. 2011b) and the historical reference period is 1978-1997.*

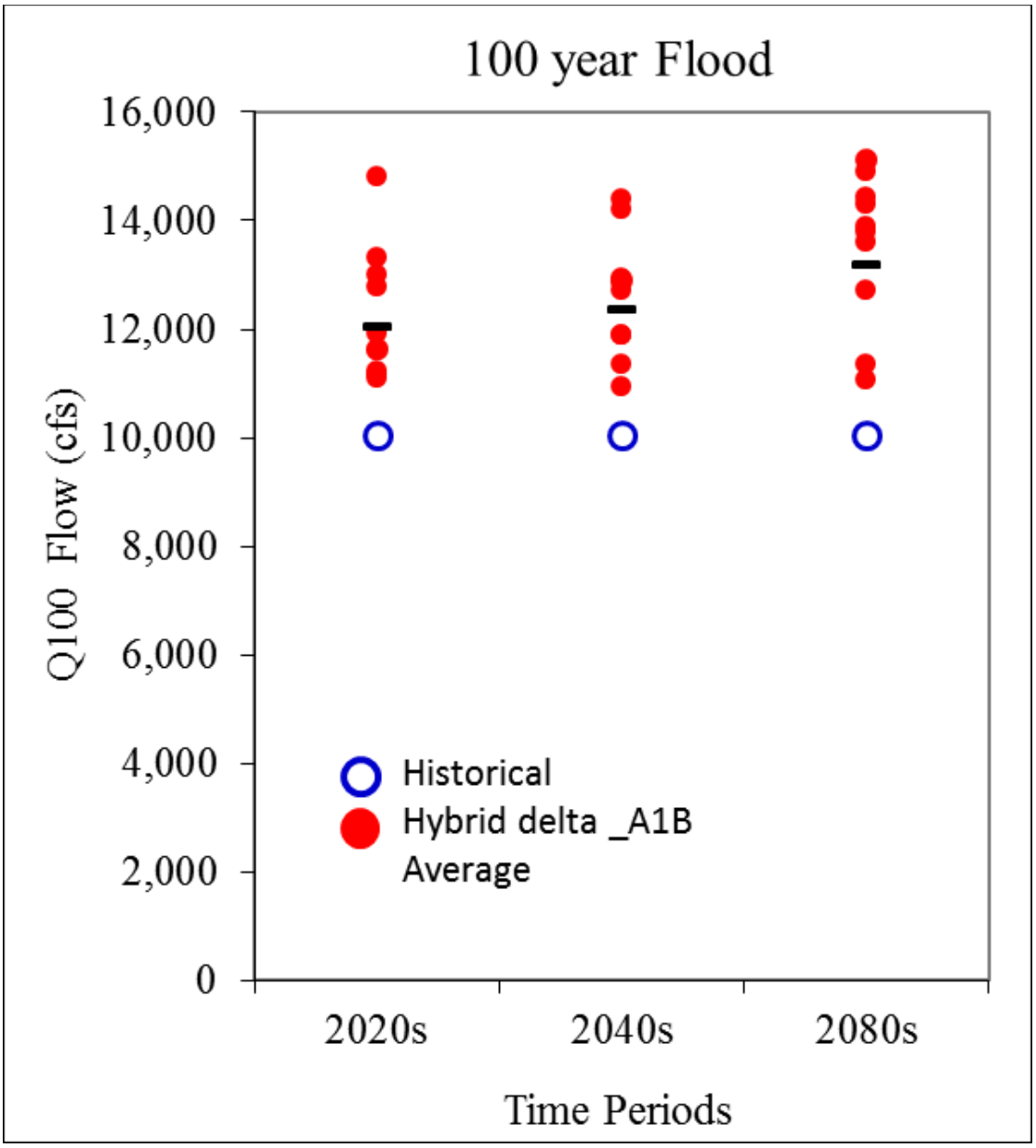

Figure B7. *Magnitude of large (100-year) floods for the Tsoo-Yess River adjacent to the Makah National Fish Hatchery based on raw Variable Infiltration Capacity (VIC) simulations for the 2020s, 2040s, and 2080s. Flows projections are based on the VIC model forced by output from an ensemble of 10 general circulation models (GCMs) under the A1B greenhouse gas emissions scenario. Red dots are the projections for the individual GCMs, the black horizontal dash (−) is the ensemble average, and the open circle is the historical frequency.*

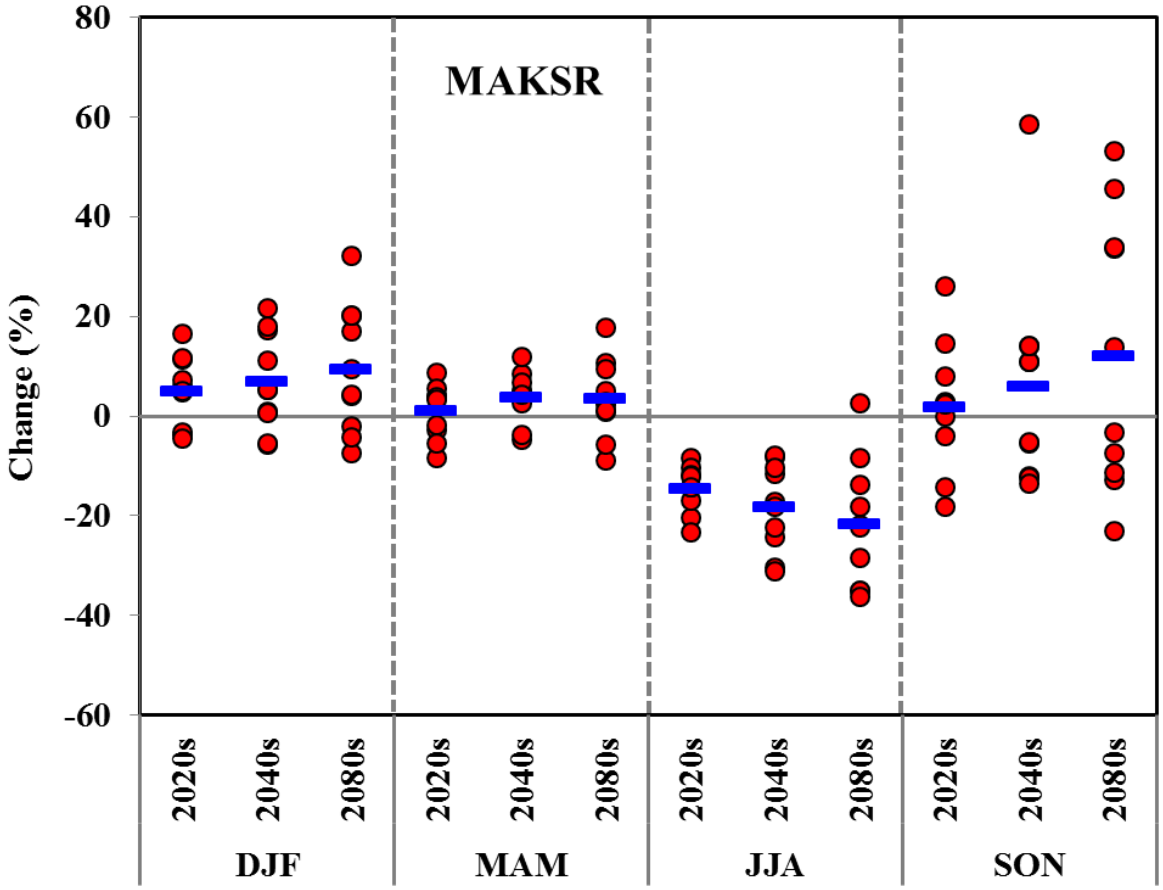

Figure B8. *Projected percent change in mean seasonal flow in the Tsoo-Yess River adjacent to the Makah National Fish Hatchery based on raw Variable Infiltration Capacity (VIC) simulations for the 2020s, 2040s, and 2080s. Flows projections are based on the VIC model forced by output from an ensemble of 10 general circulation models (GCMs) under the A1B greenhouse gas emissions scenario. Seasons depicted are winter (DJF), spring (MAM), summer (JJA), and fall (SON), where the letters denote the first initial of each month in the season.*

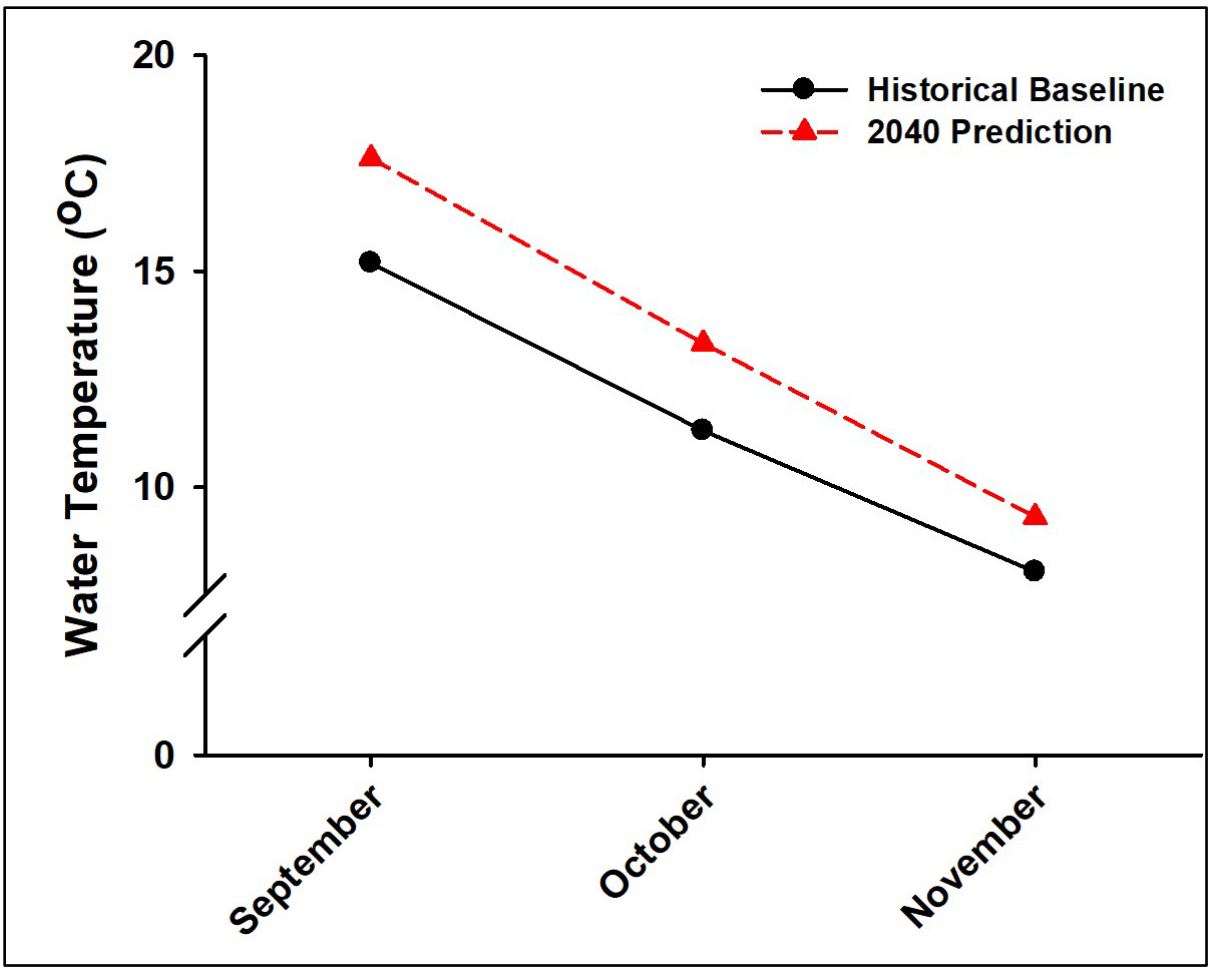

Figure B9. *Comparison of the mean water temperatures experienced by Chinook salmon broodstock held at Makah NFH based on the historical baseline (1982 – 1989) and projected values for the 2040s.*

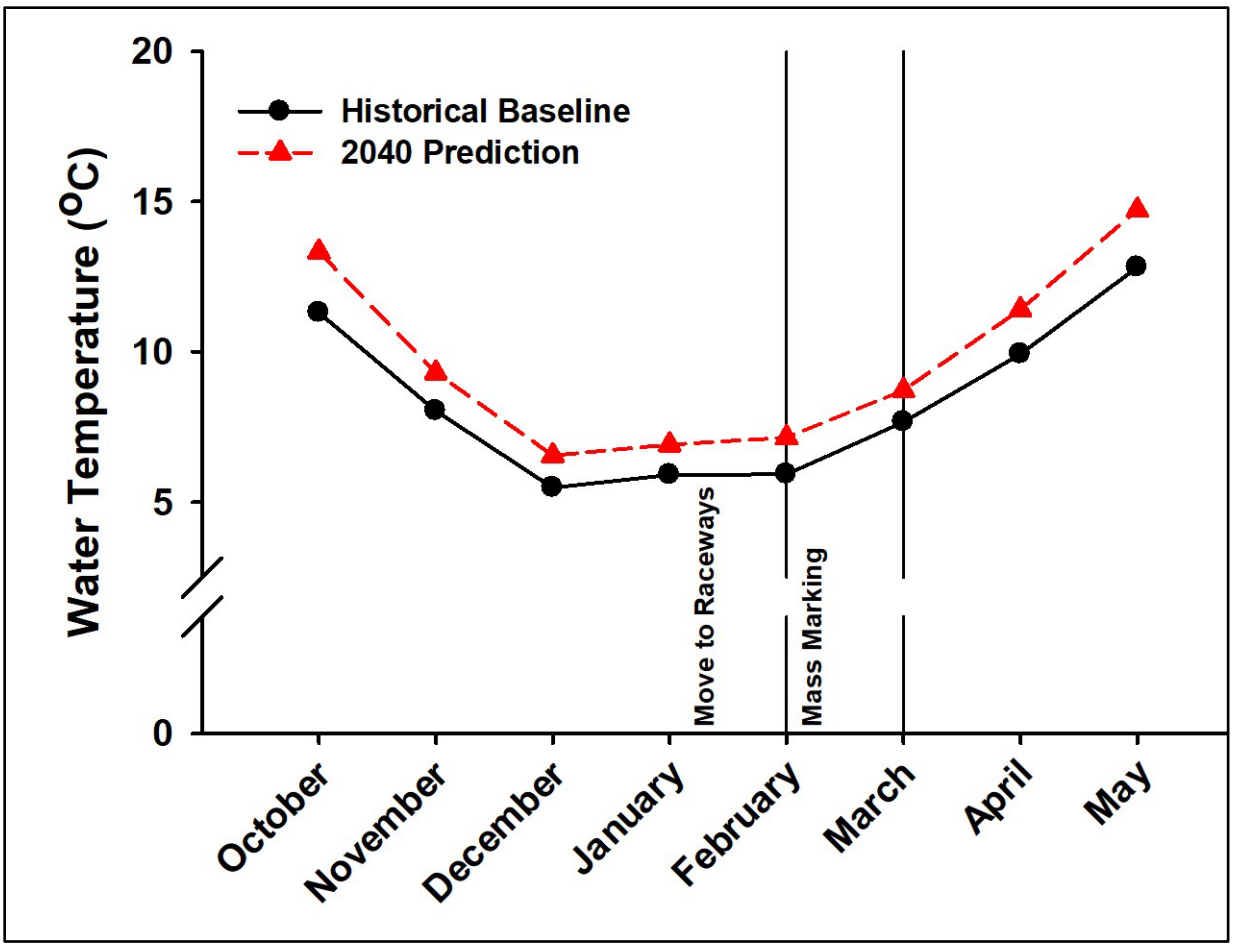

Figure B10. *Comparison of the mean water temperatures experienced by juvenile Chinook salmon reared at Makah NFH based on the historical baseline (1982 – 1989) and projected values for the 2040s. The approximate dates of important hatchery events are denoted by labeled vertical lines.*

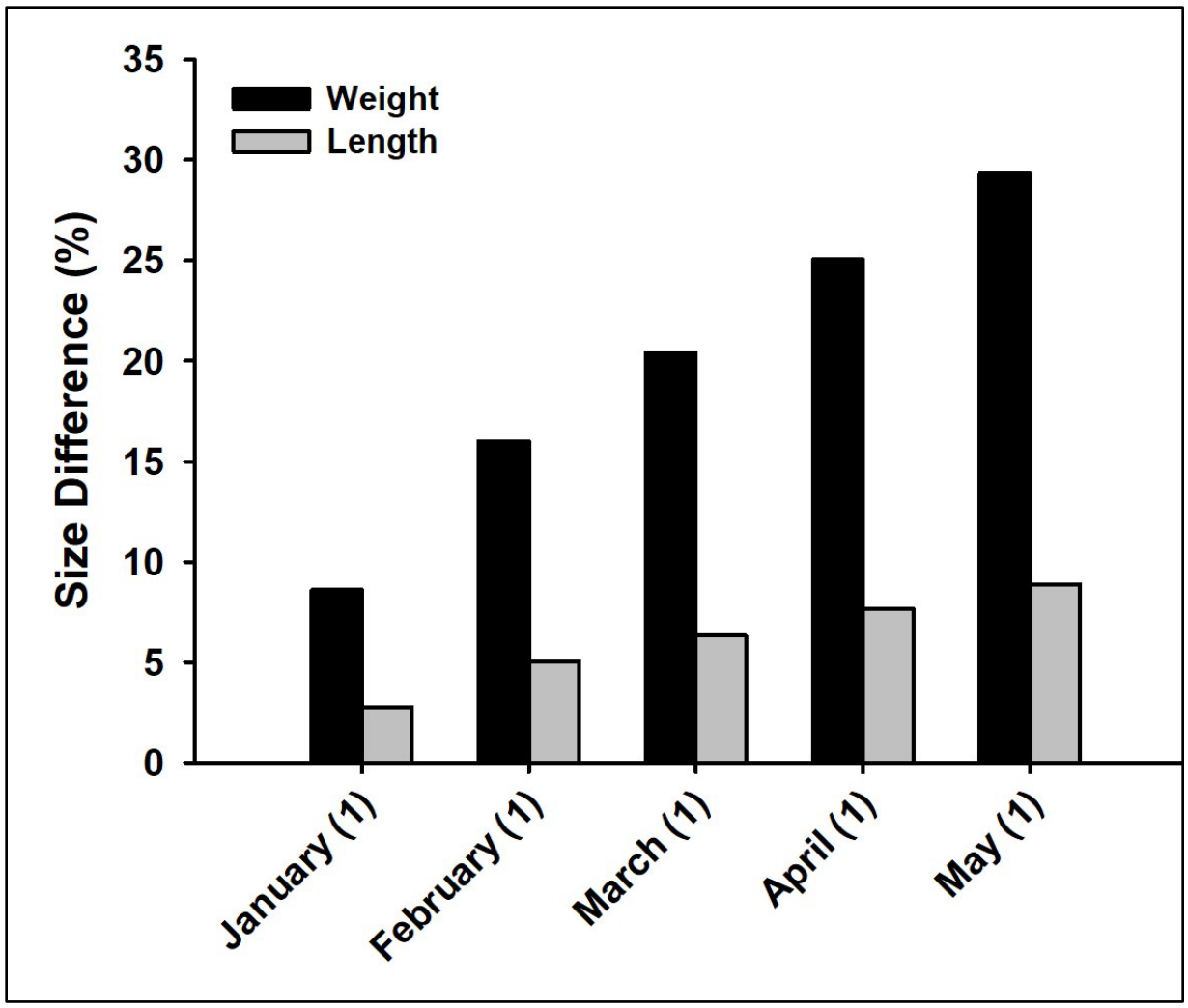

Figure B11. *Predicted monthly size differences of juvenile Chinook salmon reared at Makah NFH. Values are the simulated mean differences in weight and length of fish exposed to water temperatures predicted for the 2040s versus fish exposed the historical baseline (1982 – 1989).*

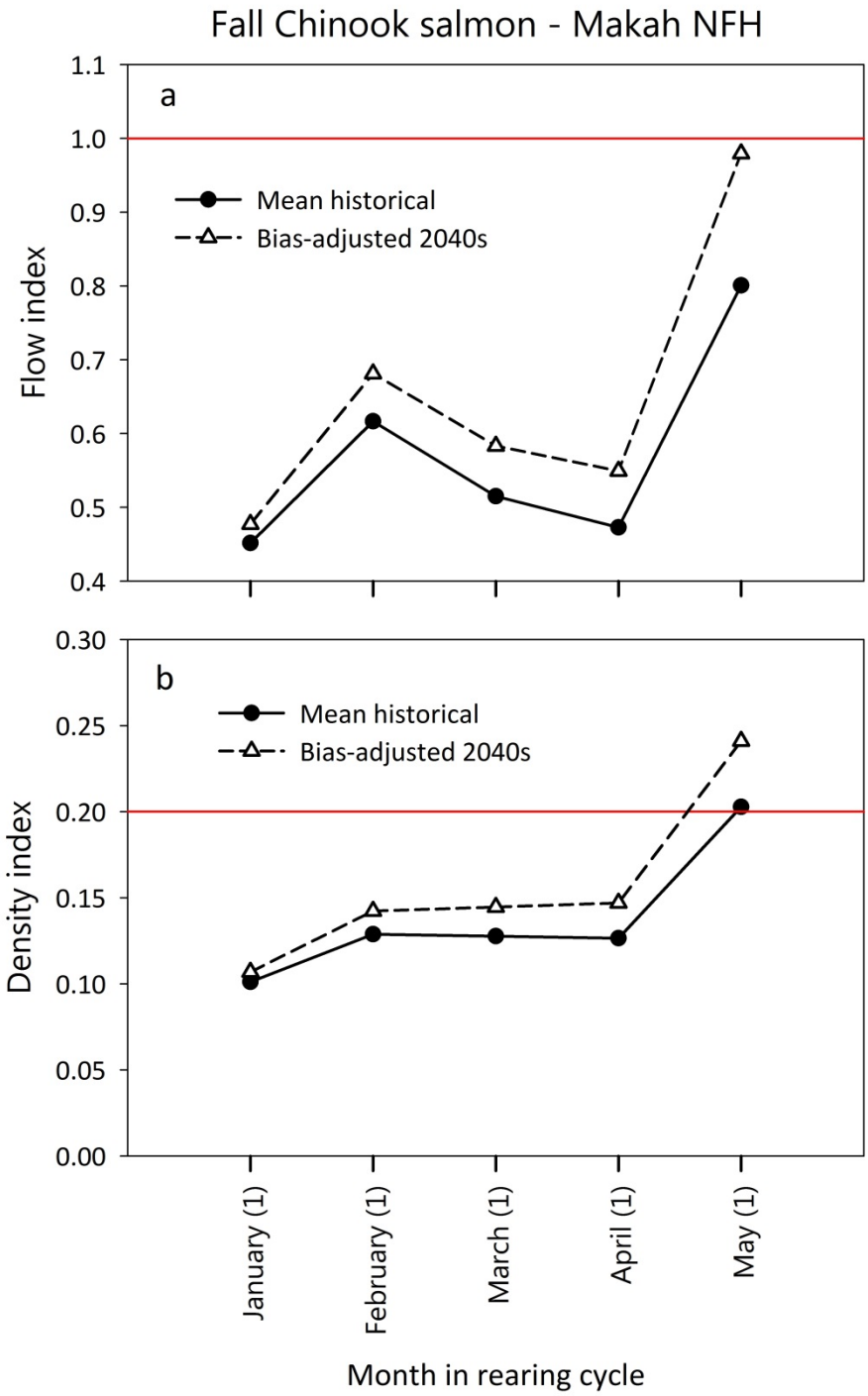

Figure B12. *Mean historical (empirical) and bias-corrected modeled future flow index (a) and density index (b) values for fall Chinook salmon at Makah National Fish Hatchery based on average rearing conditions during 2011-2014. Values for the 2040s have been bias corrected by multiplying the uncorrected future values by the ratio:* $\frac{mean\ historical\ (empirical)\ value}{modeled\ historical\ value}$. *See Table B8 for bias correction values. The horizontal lines in each plot denote the hatchery's "do not exceed" value for each index.*

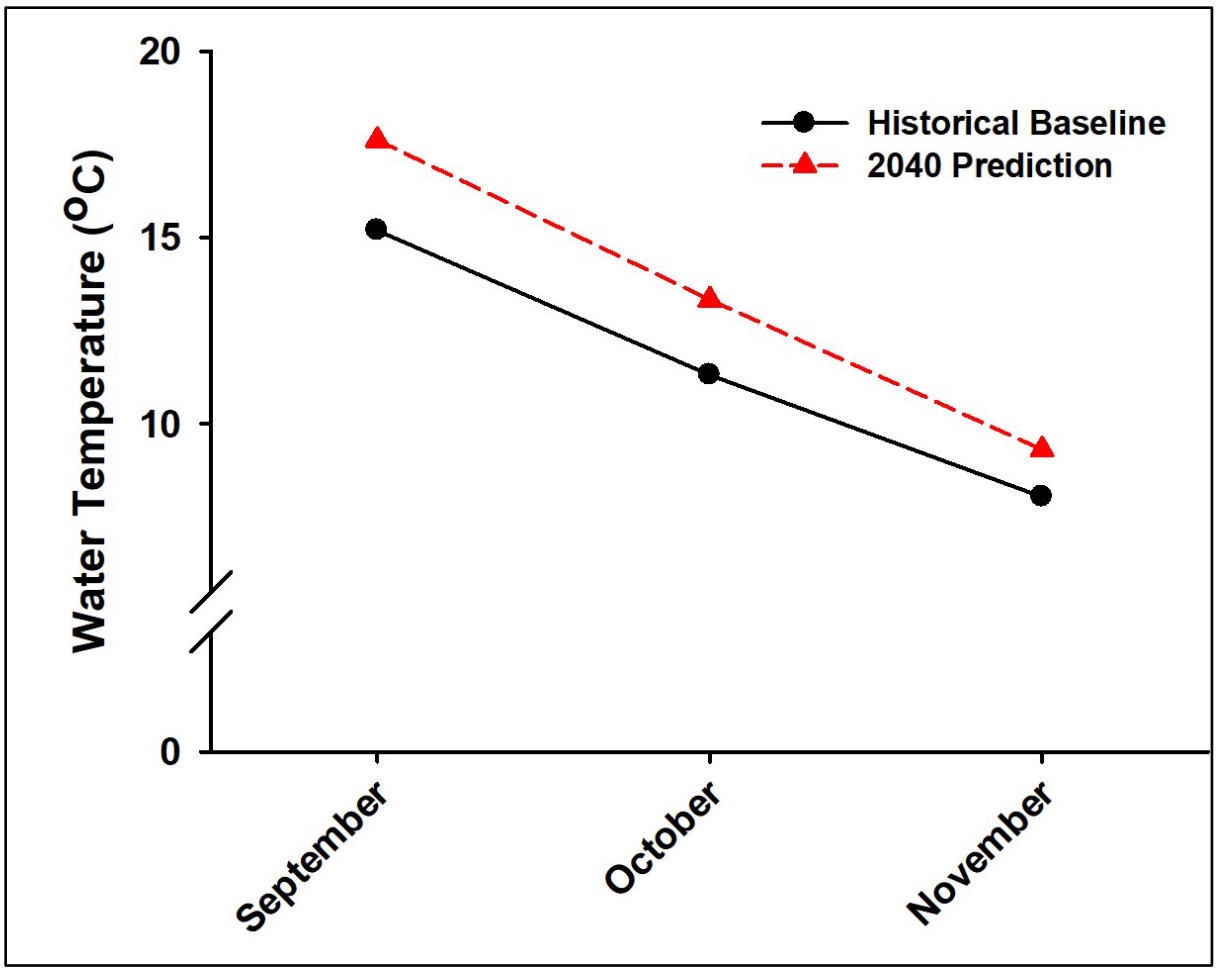

Figure B13. *Comparison of the mean water temperatures experienced by coho salmon broodstock held at Makah NFH based on the historical baseline (1982 – 1989) and projected values for the 2040s.*

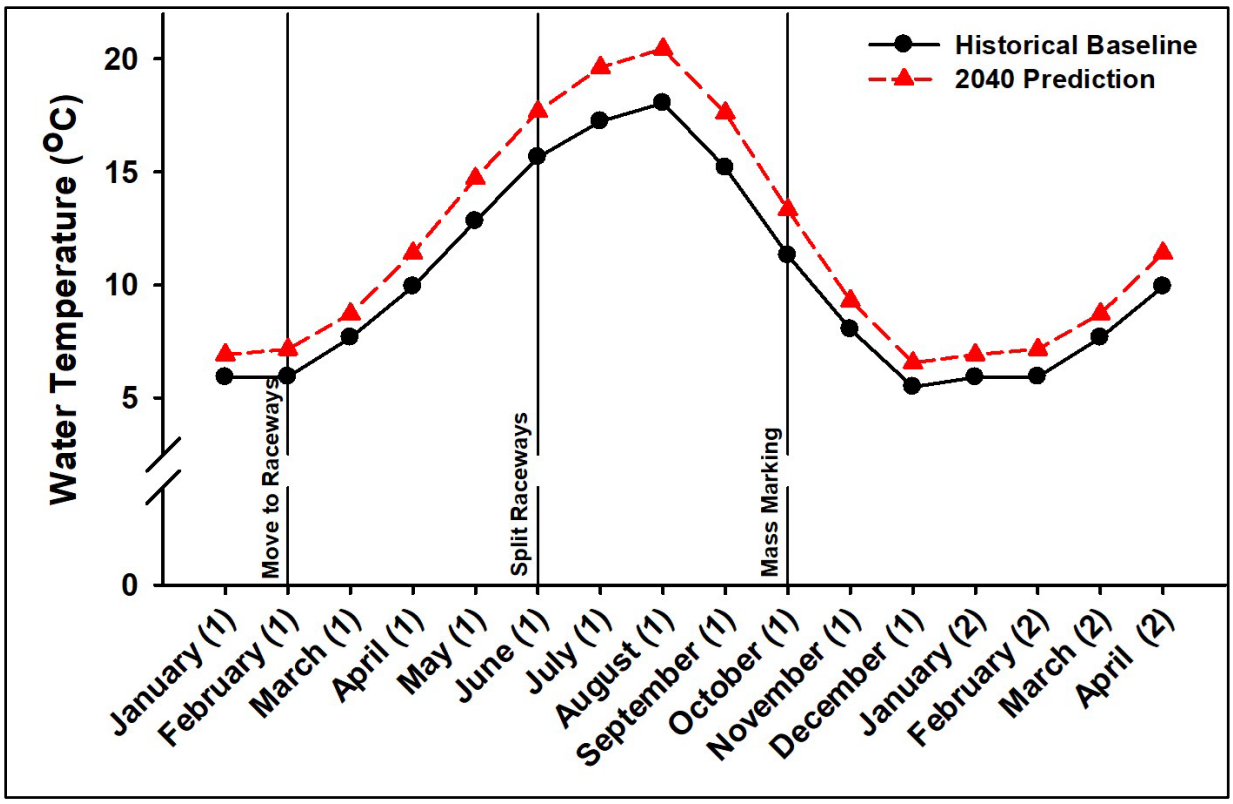

Figure B14. *Comparison of the mean water temperatures experienced by juvenile coho salmon reared at Makah NFH based on the historical baseline (1982 – 1989) and projected values for the 2040s. The approximate dates of important hatchery events are denoted by labeled vertical lines.*

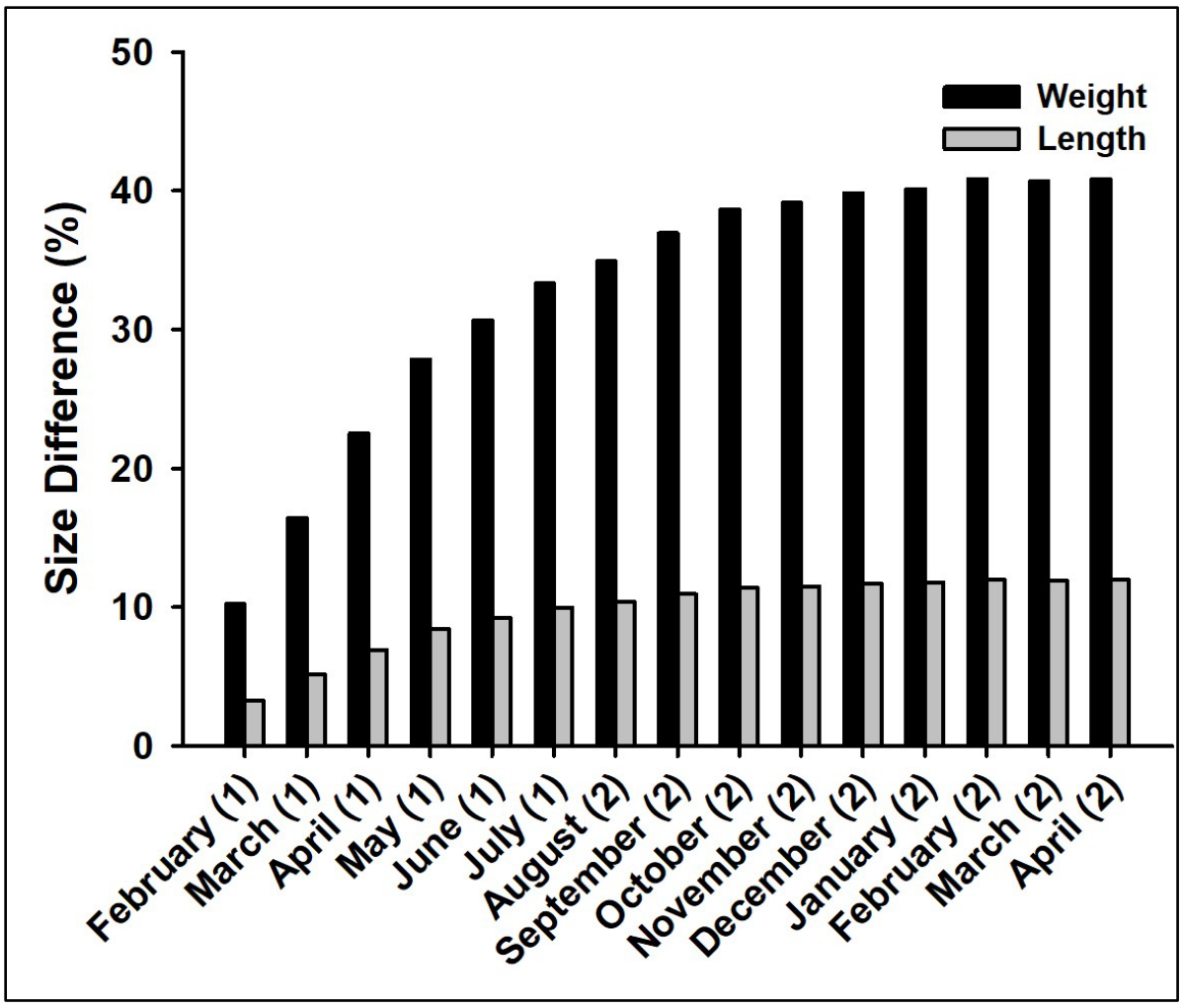

Figure B15. *Predicted monthly size differences of juvenile coho salmon reared at Makah NFH. Values are the simulated mean differences in weight and length of fish exposed to water temperatures predicted for the 2040s versus fish exposed the historical baseline (1982 – 1989).*

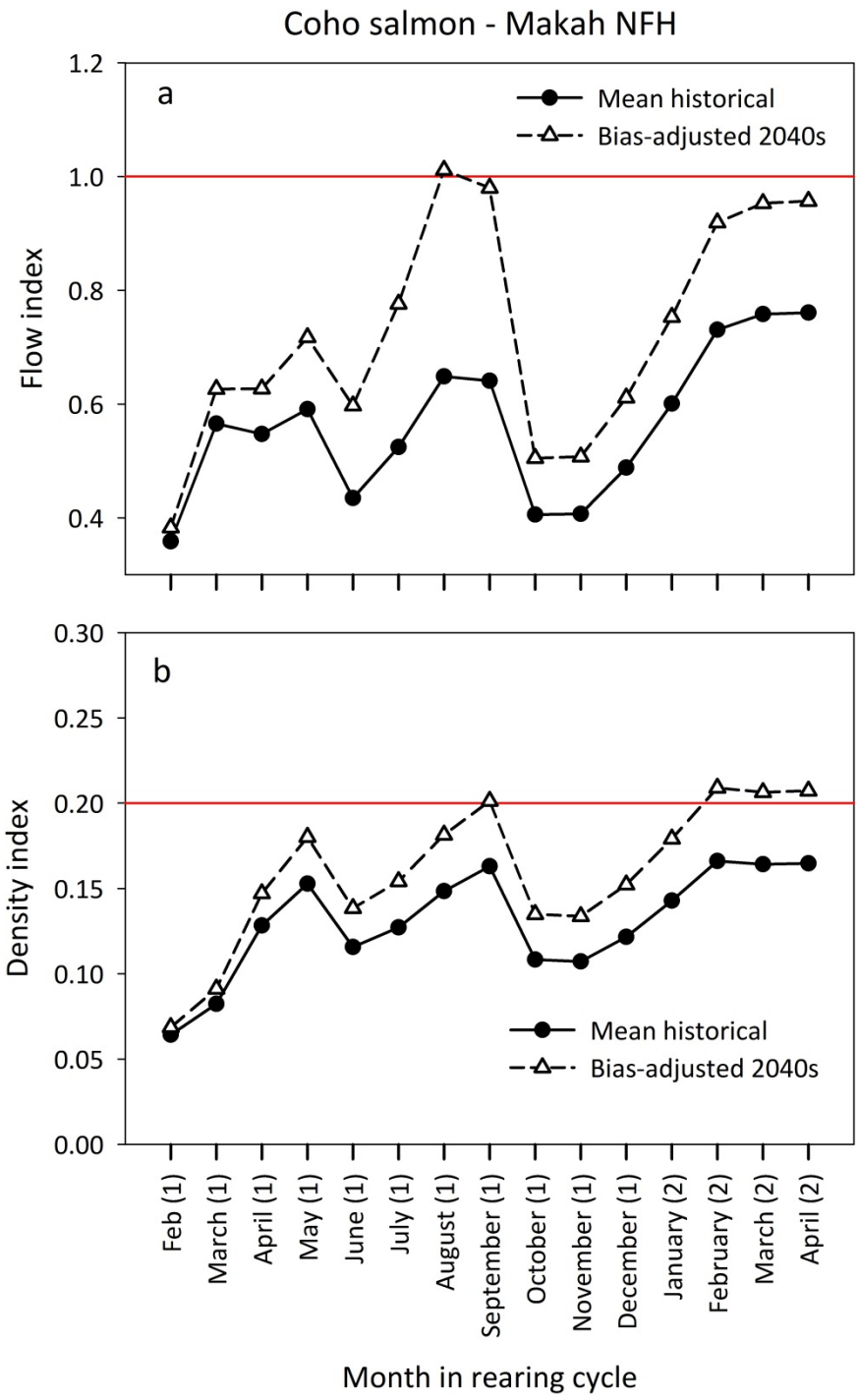

Figure B16. *Mean historical (empirical) and bias-corrected modeled future flow index (a) and density index (b) values for coho salmon at Makah National Fish Hatchery based on average rearing conditions during 2010-2013. Values for the 2040s have been bias corrected by multiplying the uncorrected future values by the ratio:* $\frac{mean\ historical\ (empirical)\ value}{modeled\ historical\ value}$. *See Table B14 for bias correction values. The horizontal lines in each plot denote the hatchery's "do not exceed" value for each index.*

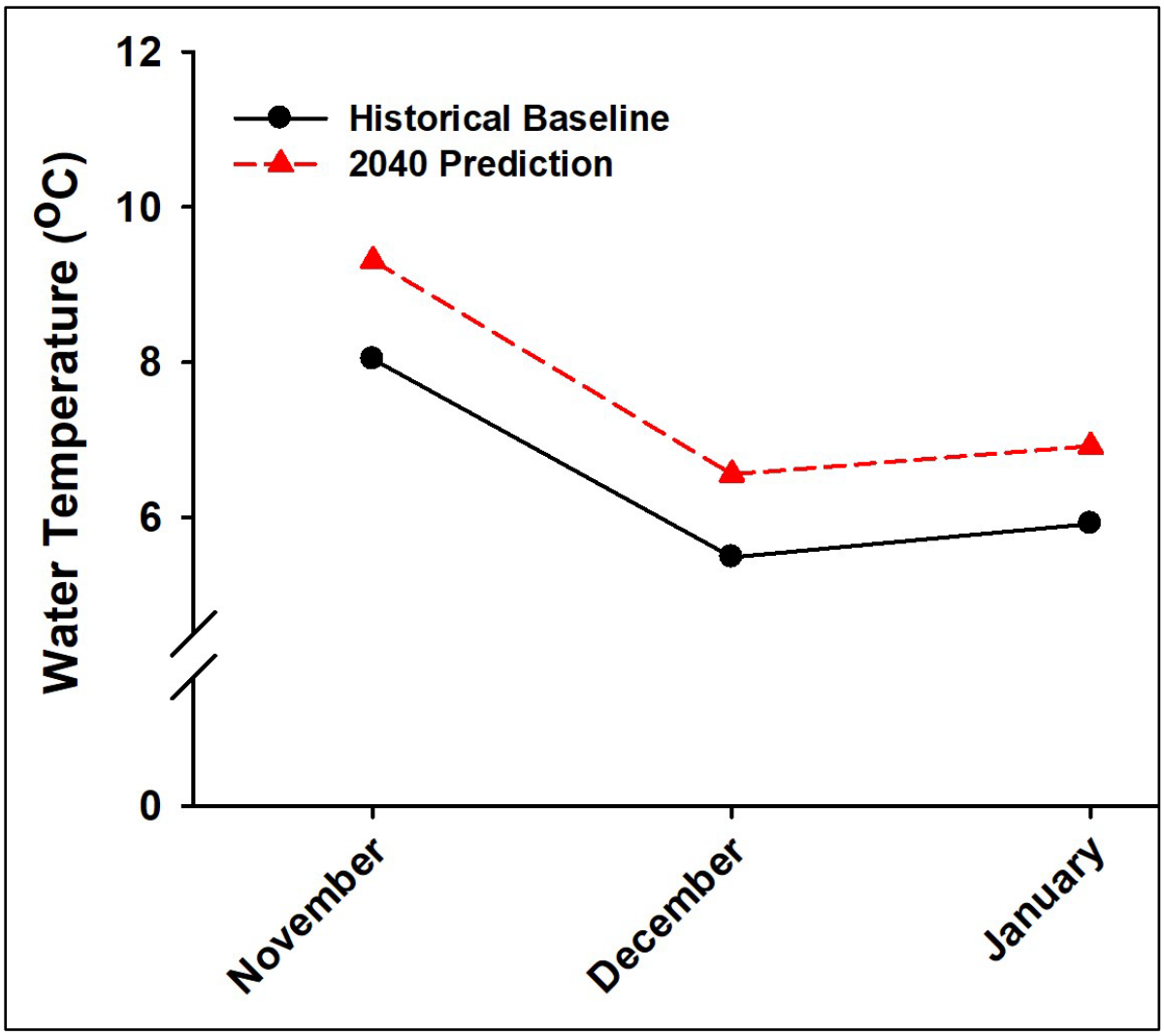

Figure B17. *Comparison of the mean water temperatures experienced by steelhead broodstock held at Makah NFH based on the historical baseline (1982 – 1989) and projected values for the 2040s.*

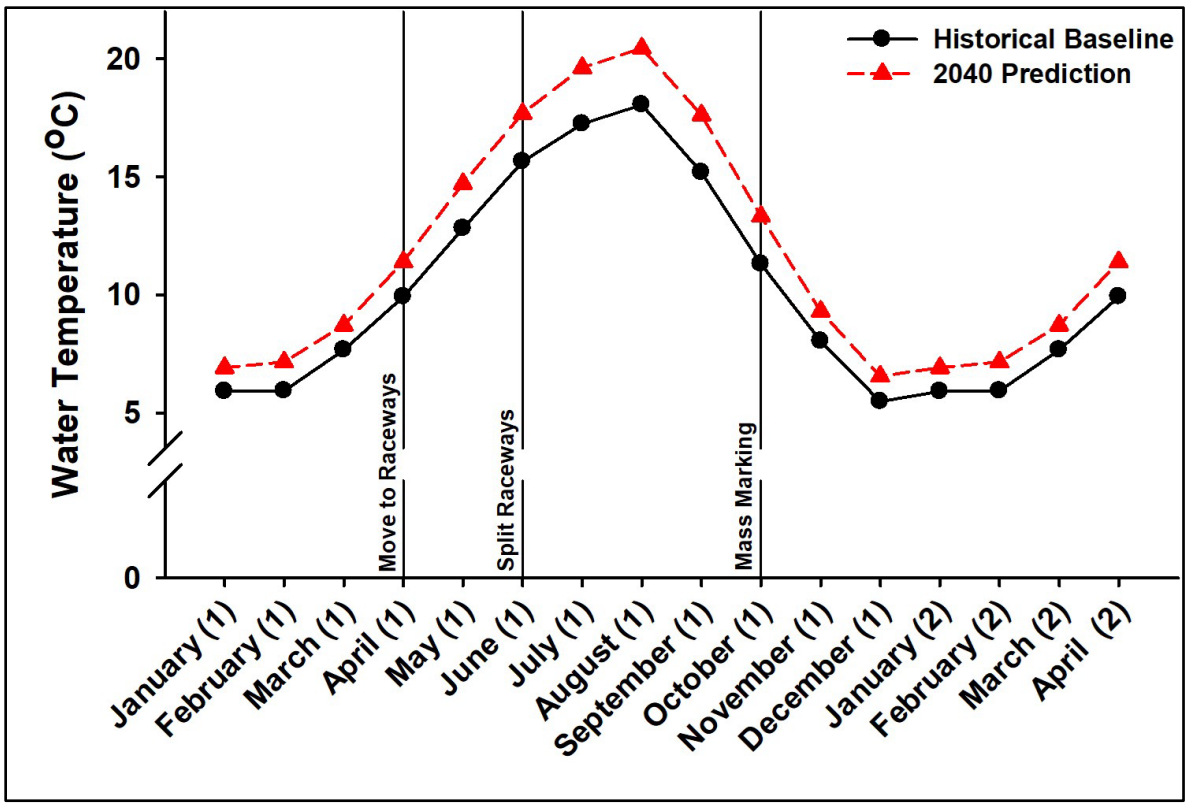

Figure B18. *Comparison of the mean water temperatures experienced by juvenile steelhead reared at Makah NFH based on the historical baseline (1982 – 1989) and projected values for the 2040s. The approximate dates of important hatchery events are denoted by labeled vertical lines.*

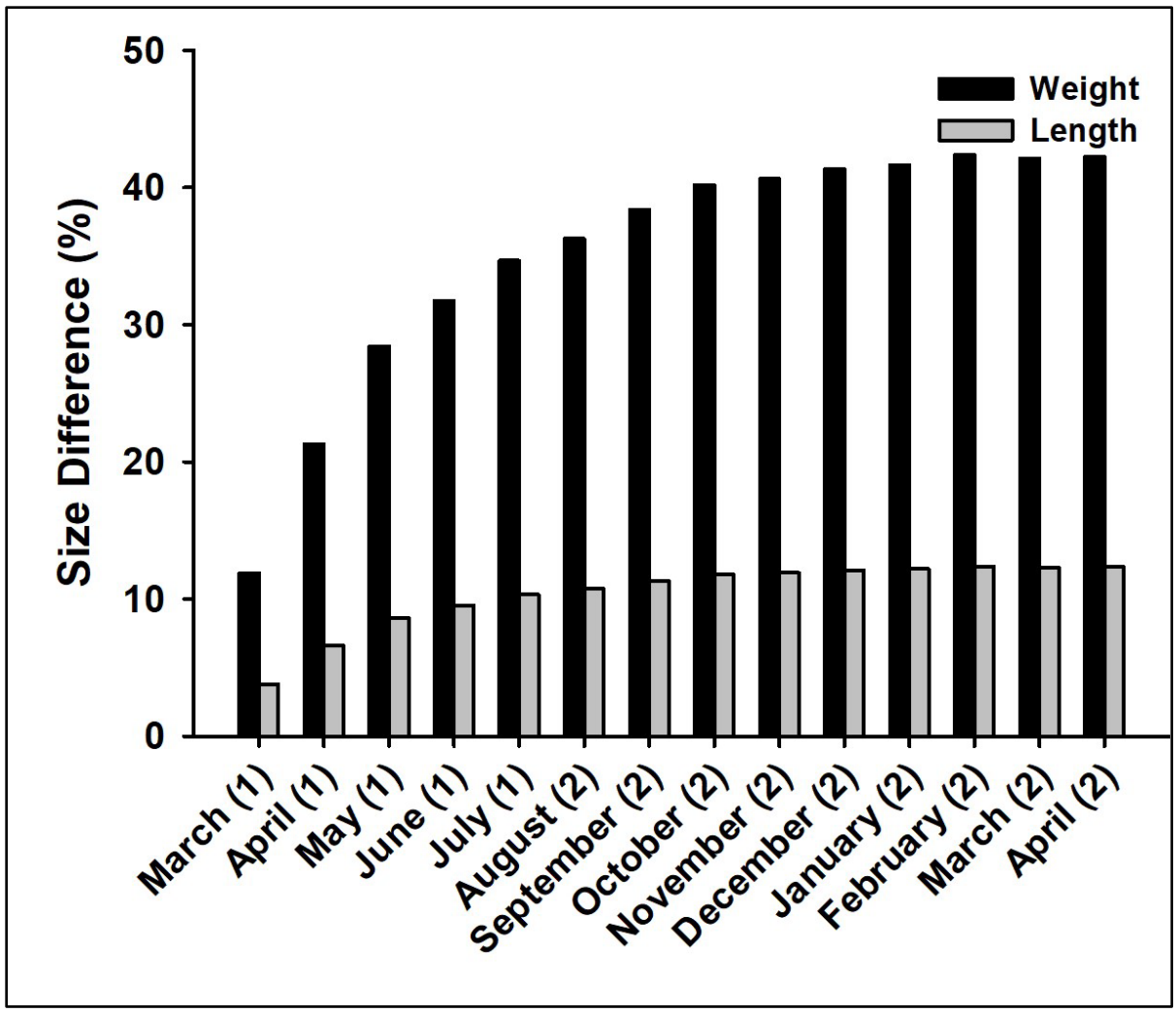

Figure B19. *Predicted monthly size differences of juvenile steelhead reared at Makah NFH. Values are the simulated mean differences in weight and length of fish exposed to water temperatures predicted for the 2040s versus fish exposed the historical baseline (1982 – 1989).*

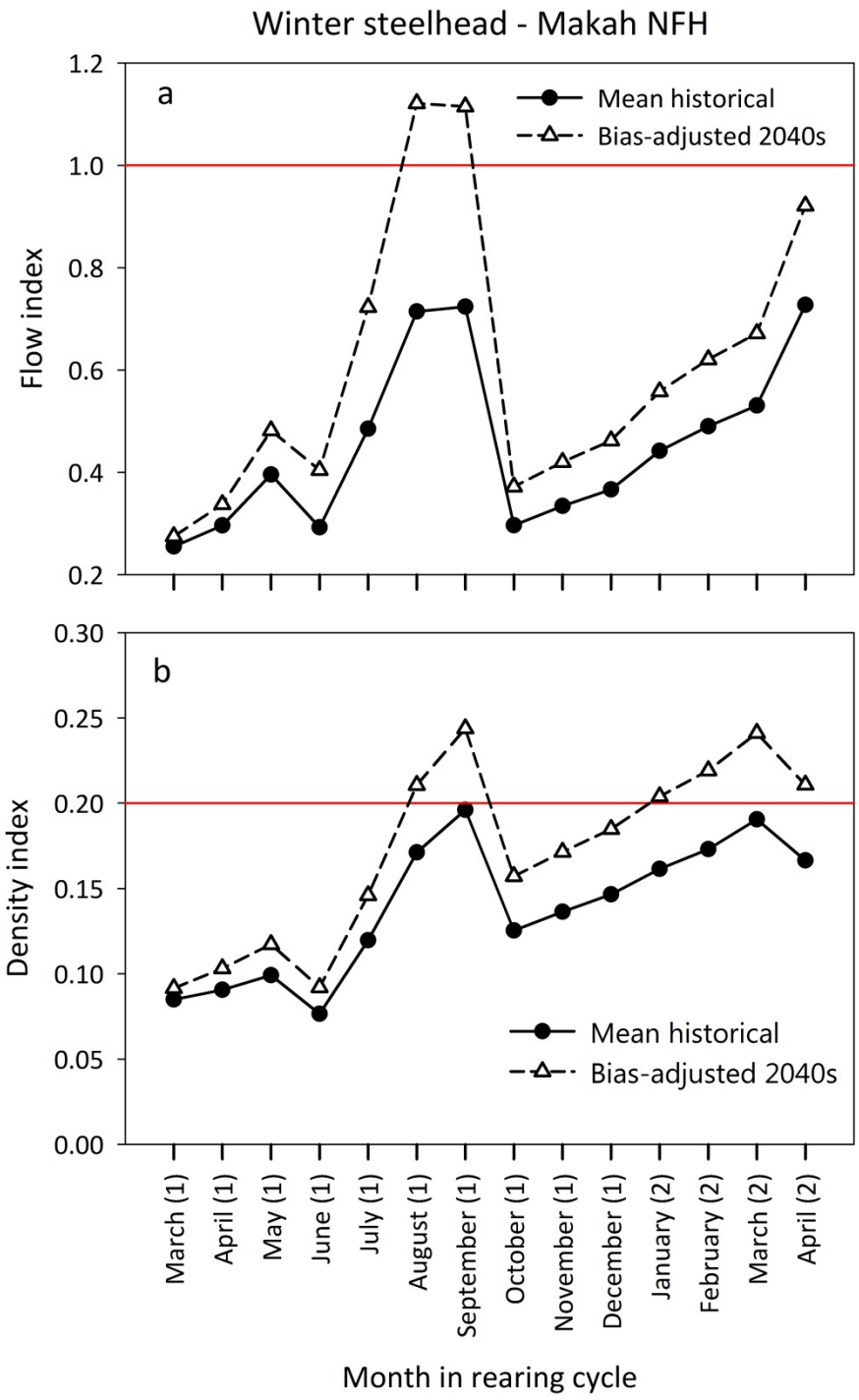

Figure B20. *Mean historical (empirical) and bias-corrected modeled future flow index (a) and density index (b) values for winter steelhead at Makah National Fish Hatchery based on average rearing conditions during 2011-2014. Values for the 2040s have been bias corrected by multiplying the uncorrected future values by the ratio:* $\frac{mean\ historical\ (empirical)\ value}{modeled\ historical\ value}$. *See Table B11 for bias correction values. The horizontal lines in each plot denote the hatchery's "do not exceed" value for each index.*

This page is blank intentionally.